Resilience Improvement of Multi-Microgrid Distribution Networks using Distributed Generation

Davoud Baghbanzadeh[1], Javad Salehi[1,*], Farhad Samadi Gazijahani[1], Miadreza Shafie-khah[2], and João P. S. Catalão[3,*]

[1]Department of Electrical Engineering, Azarbaijan Shahid Madani University, Tabriz, Iran
[2] School of Technology and Innovations, University of Vaasa, Vaasa, Finland
[3] Faculty of Engineering of University of Porto and INESC TEC, Porto, Portugal
Emails: j.salehi@azaruniv.ac.ir and catalao@fe.up.pt

Abstract

Natural disasters such as earthquakes, hurricanes, and other extreme weather events along with human sabotage attacks pose serious risks to critical infrastructures especially electrical energy systems. Hardening and operational actions are the measures to improve the resiliency of the power systems against extreme events. The long-term hardening actions strive to organize the reinforcement of power system infrastructures which accomplished at the pre-events stage. Besides, the short-term operational measures such as network reconfiguration and generation scheduling are applied to form the multiple microgrids aimed at increasing the flexibility of the power system to cope with the severe events. These measures are taken during and after the occurrence of the disasters. In this paper, an integrated framework has been proposed to increase the resiliency of distribution system. In the proposed framework, there are two models so called *defender-attacker-defender* which are made to find the best possible solution in order to reduce the load-shedding of the system during extreme events. In the first model, the hardening measures are examined at the first level to increase the robustness of the system. The worst scenarios with the highest load-shedding are calculated in the second level and subsequently reconfiguration is performed in the third level to decrease the load-shedding. In the second model, the first and second levels specify the best reinforcement plan and the worst attack scenario respectively, and in the third level, optimal distributed generation placement is accomplished to supply the demand during islanding mode of microgrids. The proposed models are organized as tri-level mixed integer optimization problem and column constraint generation algorithm is utilized to make them computationally obedient. At the end, we have implemented the suggested models on the well-known IEEE 33-bus and 69-bus systems to prove their effectiveness and applicability at improving the resiliency of the distribution systems.

Keywords: Distribution system, resilience, distributed generation, reconfiguration, microgrid.

Nomenclature

Indices and sets

i,j	index of buses
L	set of indices for branches
N	set of indices for nodes
(i,j)	index for power lines from node *i* to node *j*, iϵN , jϵN , (i,j)ϵL
IT_{up}	the iteration index of upper level problem
IT_{lp}	the iteration index of lower level problem

Parameters

B_h	budget for hardening power lines
B_a	budget for attacking power lines
GDG	number of DG units
r_{ij}, x_{ij}	resistance and reactance of power line (i,j)
$P_{L,j}$, $Q_{L,j}$	active and reactive power demands at node j
Groot	status of DG installation, $Groot_j = 1$ indicates there is DG installed at bus j, otherwise $Groot_j = 0$
R_{root}	status of root bus of the current topology, $Rroot_{,j} = 1$ indicates bus j is the current root bus; otherwise $Rroot_{,j} = 0$
$\theta(j)$, $\omega(j)$	the set of all parent buses and children buses of bus *j*
N_{bus}	Number of buses
N_{island}	Number of islands
M,M`	large numbers for Big-M method
S_{ij}^{max}	Permissible limit of power passing through the lines
P_{DG}^{max}, P_{DG}^{min}	Maximum and minimum active powers of DG
Q_{DG}^{max}, Q_{DG}^{min}	Maximum and minimum reactive powers of DG
U^{max} ,U^{min}	Maximum and minimum levels for voltage of buses

Variables

z	decision binary variable for hardening programs
v	decision binary variable for attack plans
γ	decision binary variable for root bus status
w	decision binary variable for reconfiguration programs

DG	binary variable for DG installation, DG_j=1 means a DG installed in bus j, otherwise DG_j=0
q	Dummy binary variable
qq	dummy binary variable
φ,ψ	dummy binary variables
P_{shed}	active load curtailment
Q_{shed}	reactive load curtailment
P_{DG}	active DG output power
Q_{DG}	reactive DG output power
H	the active power flow on distribution line
G	the reactive power flow on distribution line
U	the bus voltage amplitude
F	fictitious load at each bus
α	first level variable coefficient
β	second level variable coefficient
η	second level dual variable
μ	Second level linearization variables

Calculation operator

f(η)	second level dual function
C[.]	Returns 0 when input is 0, otherwise returns 1

1. Introduction

1.1 Concepts

Around the world, the planning and operation of power system infrastructures are generally done based on security and adequacy requirements. These principles allow the system structure to withstand known threats to supply customer demands with a high quality and minimal disruption over a long period of time.

In recent years, due to climate change the number and severity of natural disasters such as storms, floods, droughts, etc., have been increased in most countries. As a result, this issue is becoming more and more apparent that considerations beyond the principles of reliability for power supply is needed. In 2012, northeastern states of USA were hit by the Hurricane Sandy that destroyed about 100,000 electrical cables. These events cut off power to about 7 million people. Due to the continuous increase in greenhouse gas concentrations, the frequency, severity and duration of severe weather events are expected to increase [1].

Such power outages highlight the fact that power systems urgently need additional capabilities and practical solutions to withstand such unusual events, which have a major impact on social commitments. Thus, in recent years, the concept of resilience has been introduced as a complement to previous concepts to ensure the optimal operation of the power system in these situations. A resilient system is able to effectively take the necessary steps to mitigate the effects of such events. There are several definitions of the concept of resilience. System resilience is an ability to prepare and adapt to changing conditions, resistance and rapid return of disorders. This definition includes all active and passive aspects of this concept [2].

The special features of distribution networks have made resilience in these networks more influenced by smart network technology. For example, in a distribution network that does not include any microgrids in normal operation and the microgrids come into after disasters, the return part of resiliency is more important. In fact, in distribution systems, due to the simple and radial structure of the network and the heterogeneous geographical distribution of subscribers with different priority rights, it is possible to prevent the spread of fault only by spending a lot of money. On the other hand, in a distribution network that has multiple microgrids connected to the network, the load balance between microgrids in potential times, with proper use of pre-accident measures such as charging storage or reducing loads by demand response programs is achieved. In other words, resilience in distribution networks can only be achieved by exploiting the microgrid [3]. The concept of resilience is different from reliability. Conceptually, the reliability is the system's ability to provide a sufficient level of power to customers permanently. The main differences between reliability and resilience are summarized in Table 1 [1].

Table 1. Reliability versus Resilience

Reliability	**Resilience**
High probability, low impact	Low probability, high impact
Static	Adaptive, ongoing, short and long term
Evaluates the power system states	Evaluates the power system states and transition times between states
Concerned with customer interruption time	Concerned with customer interruption time and the infrastructure recovery time

1.2. Literature Review

The application of two-level programs for vulnerability analysis of power systems under multiple contingencies has examined in [4]. A minimum vulnerability model and a maximum vulnerability model are presented and discussed. In both models, the upper-level optimization determines a set of simultaneous outages in the transmission network whereas the lower-level optimization models the reaction of the system operator against the outages identified in the upper level. The system operator reacts by minimizing the system load shed through an optimal operation of the power system. Two solution approaches for the resulting mixed-integer non-linear bi-level programs are analyzed and compared.

A two-stage programming based on stochastic mixed-integer program with damage scenarios has been provided in [5] considering natural disasters as a set of stochastic events. The tractability of an exact and several heuristic algorithms based on decompositions that are hybrids of techniques

developed by the AI and operations research communities have been developed and investigated. Microgrids with distributed generation (DG) provide a resilient solution in the case of major faults in a distribution system due to natural disasters. In [6], a novel distribution system operational approach by forming multiple microgrids energized by DG from the radial distribution system in real-time operations to restore critical loads from the power outage has been proposed. A mixed-integer linear program is formulated to maximize the critical loads to be picked up while satisfying the self-adequacy and operation constraints for the microgrids formation problem by controlling the ON/OFF status of the remotely controlled switch devices and DG.

To increase the resilience of an electric distribution system against natural disasters, a resilient distribution network planning problem (RDNP) to coordinate the hardening and distributed generation resource allocation with the objective of minimizing the system damage has been provided in [7].The problem is formulated as a two-stage robust optimization model. Hardening and distributed generation resource placement are considered in the distribution network planning. One of complementary value propositions of microgrids is to improve power system resiliency via local supply of loads and curtailment reduction. This subject is investigated in [8] by proposing a resiliency-oriented microgrid optimal scheduling model. The proposed model aims at minimizing the microgrid load curtailment by efficiently scheduling of available resources when supply of power from the main grid is interrupted for an extended period of time. The problem is decomposed to normal operation and resilient operation problems.

A resilience-oriented service restoration method using microgrids to restore critical load after natural disasters is proposed in [9]. Considering the scarcity of power generation resources, the concept of continuous operating time is introduced to determine the availability of microgrids for critical load restoration and assess the service time. A robust optimal line hardening method coupled with multiple provisional microgrids to improve the distribution system resilience against worst N-k contingencies has been examined in [10]. A tri-level optimal model is considered with the objectives of minimizing the costs of line hardening and the operation of multiple islanded provisional microgrids, which could include the cost of load shedding in each provisional microgrid considering the worst N-k contingencies.

The concept of resiliency and its dimensions in distribution networks has been addressed in [2]. A model based on mixed-integer linear programming is proposed to properly model and evaluate the resiliency of smart distribution systems. In the proposed model, optimal formation of dynamic microgrids (MGs), their service areas, and the optimal management of different technologies such as energy storage (ES) units, demand side management programs and distributed generations (DGs) units are investigated. In addition, employing a two-stage framework based on stochastic programming, the impact of increasing penetration level of the renewable energy resources and their related uncertainties on system resiliency is examined.

Power system resilience includes hardening measures and operational restoration measures. These two aspects of resilience measures are innovatively combined in [11] to improve power system resilience. According to reviewed papers in above, Table 2 can be presented in order to clarify comparing different between reviewed papers.

Table 2. Taxonomy of the recent paper applied on the proposed problem

Ref.	Model	Description
[4]	Mixed-integer non-linear bi-level programs	The upper-level optimization determines a set of simultaneous outages in the transmission network whereas the lower-level optimization models the reaction of the system operator against the outages identified in the upper level
[5]	Two-stage, stochastic mixed-integer program	An optimal electrical distribution grid design problem as a two-stage, stochastic mixed-integer program with damage scenarios from natural disasters modeled as a set of stochastic events has been formulated
[6]	Mixed-integer linear program	A novel distribution system operational approach by forming multiple microgrids energized by DG from the radial distribution system in real-time operations to restore critical loads from the power outage has been proposed
[7]	Two-stage robust optimization model	A resilient distribution network planning problem (RDNP) to coordinate the hardening and distributed generation resource allocation with the objective of minimizing the system damage has been provided
[8]	Two stage of normal operation and resilient operation problems	The proposed model aims at minimizing the microgrid load curtailment by efficiently scheduling of available resources when supply of power from the main grid is interrupted for an extended period of time
[9]	Two-stage heuristic program	A resilience-oriented service restoration method using microgrids to restore critical load after natural disasters has proposed
[10]	Tri-level optimal model	A tri-level optimal model is considered with the objectives of minimizing the costs of line hardening and the operation of multiple islanded provisional microgrids, which could include the cost of load shedding in each provisional microgrid considering the worst N-k contingencies
[2]	Mixed-integer linear program	A model based on mixed-integer linear programming is proposed to properly model and evaluate the resiliency of smart distribution systems.
[11]	Tri-level defender-attacker-defender (DAD) model	Power system resilience includes hardening measures and operational restoration measures are innovatively combined to improve power system resilience

In particular, a collaborative two-stage robust model has been used in [12] to determine the power transactions between the coupled MGs to achieve the economic interests. The planning of micro-turbines and WT has been done in [13] based on probability-weighted robust optimization. In this paper, the uncertainty pertaining to variable generation has been taken into account by scenario-based approach. A bi-level interactive algorithm based on Stackelberg strategy is extended in [14] to schedule the day-ahead energy management of distribution systems associated with MGs, where the DSO is master and MGs are followers. Zhang *et al*. [15] proposed a robust two-stage operational model to effectively dispatch various converters within the multi-energy MGs considering price-based DRP and indoor temperature control. An adaptive robust optimization framework has been suggested in [16] to optimally manage the hybrid AC/DC MGs regarding to the mutual interaction between AC and DC MGs, aimed at acquiring a robust decision for hybrid AC/DC MGs. To address the uncertainties pertaining to renewables, Ref. [17] presented a min-max-min model to operate AC/DC MGs in the islanding mode considering the degradation of energy storage. In this work, the

startup/shutdown state of DGs is determined in the first stage (i.e., unit commitment), while the main objective of second stage is to dispatch the DG units (i.e., economic dispatch). Qiu *et al.* [18] expanded a multiple-time-scale rolling horizon optimization for intraday operation of AC/DC MGs by means of a distributionally robust optimization method.

According to these literatures, MG, DGs, hardening and restoration programs are the key words in the resiliency studies. Although various works have been reported various methods on the resiliency of distribution system, the combination and coordination of these instruments have not investigated properly. To address this significant gap, we proposed a novel tri-level framework to evaluate the impact of MG clustering and distributed energy resources with reconfigurable structure on the resiliency of the distribution system.

1.3. Contribution

Reinforcement programs, reconfiguration, and optimal DG placement have been keywords in recent studies in the field of resilience. In this paper, two models are considered to increase the resilience of the distribution network against extreme events. In the first model, a three-level framework is performed to increase the system resilience by considering reinforcement and reconfiguration programs. In the second model, a three-level model with reinforcement programs and optimal placement of DG resources is examined. In both models, 5 different attack scenarios are considered. Actually, the proposed models find the worst possible attack scenario, and then it optimally applies optimal reconfiguration programs and generation scheduling to deal with the event.

1.4. Paper organization

The remainder of this paper is organized as follows: section 2 formulated the mathematical form of objective function with operation constraints and radiality constraints. The solution procedure are introduced in section 3. Section 4 present the case study and the simulation results and the section 5 concludes the paper.

2. Mathematical formulation

2.1 Objective function

In this part, three stages of DAD problem (hardening, attack and restoration stages) have presented. We defined four binary variables (z, v, γ, w) to execute of our planning. So the binary decision variable z displays the hardening plans (level 1), the binary decision variable v shows the attacks that the system has suffered (level 2) and the binary decision variables γ and w represent the DG island and line reconfiguration decisions. We calculate the resilience of the case study with the sum of the load shedding. So, the objective function has presented as follows:

$$\min_{z \in L} \max_{v \in L} \min_{\substack{w \in L \\ \gamma \in N}} \min_{\{P_{sehd,j}, Q_{shed,j}, P_{DG}, Q_{DG}, H, G, U, F\}} \sum_{j \in B} P_{shed,j} \quad (1)$$

The main aim of this objective function is to minimize the curtailed loads during event by employing DG and network reconfiguration. The binary decision variable of q_{ij} specifies the terminal status of

the lines. The amount of this variable has determined by hardening, attack and reconfiguration variables that formulated below.

$$q_{ij} = w_{ij}.(z_{ij} + v_{ij} - z_{ij}.v_{ij}) \qquad ,\forall (i,j) \in L \qquad (2)$$

Where z_{ij} =0 or 1 demonstrates that the line *ij* is not hardened or hardened respectively, v_{ij} = 0 or 1 implies that the line *ij* is attacked or not attacked via natural disasters respectively and w_{ij} = 0 or 1 represents that by reconfiguration the line *ij* is opened or closed by the system operator. For simplicity, we make a dummy binary variable *qq*, so:

$$qq_{ij} = z_{ij} + v_{ij} - z_{ij}.v_{ij} \qquad ,\forall (i,j) \in L \qquad (3)$$

When qq_{ij} = 0 demonstrates that this line is not hardened and influenced by attacks and qq_{ij} = 1 means that this line is hardened or not influenced. Equation (3) demonstrates that with the hardening of the line *ij*, whether this line is attacked or not attacked, it has not influenced by the attack, but by reconfiguration this line is still can opened, so the ultimate condition of the power lines is determined by the following equation:

$$q_{ij} = w_{ij}.qq_{ij} \qquad ,\forall (i,j) \in L \qquad (4)$$

The above equations are nonlinear, so the following equations is presented for linearization:

$$\begin{cases} qq_{ij} \geq z_{ij} \\ qq_{ij} \geq v_{ij} \\ qq_{ij} \leq z_{ij} + v_{ij} \end{cases} \quad \begin{cases} q_{ij} \leq qq_{ij} \\ q_{ij} \leq w_{ij} \\ q_{ij} \geq qq_{ij} + w_{ij} - 1 \end{cases} \qquad ,\forall (i,j) \in L \qquad (5)$$

2.2 Operational constraints

In this paper, for the sake of convexity we use a linearized *DistFlow* model borrowed from [19] for power flow problem in the presence of DG units. The equations related to these constraints are presented below:

$$\begin{cases} \sum_{s \in \omega(j)} H_{js} - \sum_{i \in \theta(j)} H_{ij} = P_{DG,j} - (P_{L,j} - P_{shed,j}) \\ \sum_{s \in \omega(j)} G_{js} - \sum_{i \in \theta(j)} G_{ij} = Q_{DG,j} - (Q_{L,j} - Q_{shed,j}) \end{cases} \qquad ,\forall j \in N \qquad (6)$$

$$\begin{cases} U_i - U_j - (\frac{r_{ij}.H_{ij} + x_{ij}.G_{ij}}{U_0}) \leq M.(1 - q_{ij}) \\ U_i - U_j - (\frac{r_{ij}.H_{ij} + x_{ij}.G_{ij}}{U_0}) \geq -M.(1 - q_{ij}) \end{cases} \qquad ,\forall (i,j) \in L \qquad (7)$$

$$\begin{cases} -S_{ij}^{\max}.q_{ij} \le H_{ij} \le S_{ij}^{\max}.q_{ij} \\ -S_{ij}^{\max}.q_{ij} \le G_{ij} \le S_{ij}^{\max}.q_{ij} \end{cases} \quad ,\forall (i,j) \in L \tag{8}$$

$$\begin{cases} 0 \le P_{shed,j} \le P_{L.j} \\ 0 \le Q_{shed,j} \le Q_{L.j} \end{cases} \quad ,\forall j \in N \tag{9}$$

$$\begin{cases} P_{DG,j}^{\min} \le P_{DG,j} \le P_{DG,j}^{\max} \\ Q_{DG,j}^{\min} \le Q_{DG,j} \le Q_{DG,j}^{\max} \end{cases} \quad ,\forall j \in N \tag{10}$$

$$U_j^{\min} \le U_j \le U_j^{\max} \quad ,\forall j \in N \tag{11}$$

where the linearized DistFlow model are shown in Eq. (6) and Eq. (7). The permissible active and reactive line flow are presented in Eq. (8). The amount of active and reactive load curtailment are restricted by Eq. (9). The permissible active and reactive production of DGs are presented in Eq. (10) and the allowed range of the buses voltage are expressed in Eq. (11).

2.3 Radiality constraints

In order for a network to be operated radially, the following two conditions must be satisfied simultaneously [20]: (a) the number of closed branches equals the number of buses minus the number of islands, and (b) the connectivity of each island is guaranteed. In this paper, we pursue a single-commodity flow method from [21],[22] to be sure that the distribution system preserve the radial structure. According to the single-commodity flow method, the first condition of the radial distribution system is formulated as follow:

$$\sum_{ij \in L} q_{ij} = N_{bus} - N_{island} \tag{12}$$

The left side of the Eq.(12) represents all the closed network lines, N_{bus} is the total number of bus, and N_{island} is the number of islands in the system. To establish the second condition of the radial distribution system, we model a fictitious system with the same topology. In this fictitious system every island has only one root bus (that called ‘‘source”) and the other buses have unit load demands (that acted as a “sink”). The fictitious network has the same topology of the real system by the same connections. Thus, the satisfaction of energy balance at each bus in the fictitious network implies that at least one path exists between the ‘‘source” bus and all other buses, so that the island must be

connected. By satisfying the fictitious load, the connectivity of each island is guaranteed. Accordingly the second condition has presented by the following equations:

$$\sum_{s\in\omega(j)} F_{js} - \sum_{i\in\theta(j)} F_{ij} = -1 \qquad ,j \in N \setminus R_{root} \tag{13}$$

$$-M.q_{ij} \le F_{ij} \le M.q_{ij} \qquad ,\forall (i,j) \in L \tag{14}$$

In the above constraints, F_{ij} represents the virtual power flow in the system, and θ(j) and ω(j) are the set of all parent buses and children buses of bus j. The Eqs.(12)-(14) express the all radiality constraints of the distribution system by single-commodity flow method. The detailed formulations for the situation during attack and after optimal restoration stage are presented in [11]. We also defined a binary decision variable γ to model DG islanding where $\gamma_j = 1$ means that the bus j is chosen as root bus. In the third level (reconfiguration stage), the radiality constraint is formulated as follows [11]:

$$\sum_{ij\in L} q_{ij} = N_{bus} - \sum_{j\in N} \gamma_j \tag{15}$$

$$\sum_{s\in\omega(j)} F_{js} - \sum_{i\in\theta(j)} F_{ij} \ge -1 - M.\gamma_j.(Groot_j + \varphi_j) \tag{16}$$

$$\sum_{s\in\omega(j)} F_{js} - \sum_{i\in\theta(j)} F_{ij} \le -1 + M.\gamma_j.(Groot_j + \varphi_j) \tag{17}$$

Φ is a dummy binary variable where $\varphi_j = 1$ demonstrates that bus j is at one end of one/more faulted lines. We can define this variable by the following equation:

$$\varphi_j = C[\sum_{s\in\omega(j)} (1-qq_{js}) + \sum_{i\in\theta(j)} (1-qq_{ij})] \tag{18}$$

The nonlinear $\gamma_j . \varphi_j$ in Eq. (16) and Eq. (17) can be replaced by binary variable ψ, therefore:

$$\psi_j = \gamma_j.\varphi_j \tag{19}$$

Eq.(16) and Eq.(17) therefore are transformed to:

$$\sum_{s\in\omega(j)} F_{js} - \sum_{i\in\theta(j)} F_{ij} \ge -1 - M.\gamma_j.Groot_j - M.\psi_j \tag{20}$$

$$\sum_{s\in\omega(j)} F_{js} - \sum_{i\in\theta(j)} F_{ij} \le -1 + M.\gamma_j.Groot_j + M.\psi_j \tag{21}$$

The binary variables φ and ψ are nonlinear where linearized with these functions:

$$\begin{cases} \varphi \le \sum_{s\in\omega(j)} (1-qq_{js}) + \sum_{i\in\theta(j)} (1-qq_{ij}) \\ \varphi \ge \sum_{s\in\omega(j)} (1-qq_{js})/M + \sum_{i\in\theta(j)} (1-qq_{ij})/M \end{cases} \tag{22}$$

$$\begin{cases} \psi \le \gamma \\ \psi \le \varphi \\ \psi \ge \varphi + \gamma - 1 \end{cases} \tag{23}$$

Accordingly the radiality constraints for the hardening stage and restoration stages are Eq. (5), Eq. (14), Eq. (15), and Eqs. (20)–(23).

3. Solution Algorithm

The tri-level DAD problem is a mixed integer problem and is solved by the CCG algorithm. The full procedure of CCG algorithm is presented in [23].

First Model (tri-level of hardening, attack and optimal reconfiguration programs)

Here we divide the model into three stages:

I. **First stage:** the first stage (Upper level problems) is a minimization problem. The goal of this stage is to find the best hardening plans by the given attack plans ($\hat{V}$). Once the hardening plans is obtained, the fixed amount of the hardening plans ($\hat{z}$) will be the numerical parameters in the other stages.

II. **Second stage:** the second level (the lower-level master problem) is a max problem. The aim of this level is to detect the worst-case attack plans with the given hardening plans and system topology.

III. **Third stage:** the third level (the lower-level sub problem) is a minimization problem. The objective of this level is to seek the optimal restoration plans (w and γ) with specified hardening and attack plans.

We can alter the model in Eq. (1) to the following equation:

$$\begin{array}{lll} \min & \max & \min \\ z \in L & v \in L & w \in L \\ \gamma' \in N & & \gamma \in N \\ w' \in L & & \end{array} \quad \sum_{j \in N} P_{shed,j} \quad \left\{P_{sehd,j}, Q_{shed,j}, P_{DG}, Q_{DG}, H, G, U, F\right\} \tag{24}$$

The following proceeding must be observed in order to implement the proposed algorithm:

1. In the first level the hardening plans is determined and in the third level the reconfiguration plans obtained. Whereas the topology of the system alters in these levels, so we use γ` and w` in the first level to separate these levels from each other.
2. The topology of the system is fixed in the second level and the goal of this stage is to find the worst attack scenarios.
3. The first level is determined with the attack scenarios of lower level's problems where the new sets of recourse variables and constraints is obtained in the lower level. The second level is augmented by the by the set of recursive variables and constraints for a new topology structure identified by the L-SP.

Upper level problem (Level 1)

Once the all binary variables are stabilized then the objective function will be linear. So the first level is formulated as:

$$\min_{z \in L} \quad \min_{\{P_{sehd,j}, Q_{shed,j}, P_{DG}, Q_{DG}, H, G, U, F\}} \sum_{j \in N} P_{shed,j} \tag{25}$$

$\gamma' \in N$

$w' \in L$

The general formulation of level 1:

$$\text{OF: } \min \alpha \tag{26}$$

Operational constraints:

$$\alpha \geq \sum_{j \in N} P_{shed,j}^{It_{up}} \qquad , It_{up} = 1,2,... \tag{27}$$

$$\sum_{ij \in L} z_{ij} \leq B_h \tag{28}$$

$$\begin{cases} P_{DG,j}^{It_{up}} - (P_{L,j} - P_{shed,j}^{It_{up}}) = \sum_{s \in \omega(j)} H_{js}^{It_{up}} - \sum_{i \in \theta(j)} H_{ij}^{It_{up}} \\ \qquad , It_{up} = 1,2,... \\ Q_{DG,j}^{It_{up}} - (Q_{L,j} - Q_{shed,j}^{It_{up}}) = \sum_{s \in \omega(j)} G_{js}^{It_{up}} - \sum_{i \in \theta(j)} G_{ij}^{It_{up}} \end{cases} \tag{29}$$

$$\begin{cases} U_i^{It_{up}} - U_j^{It_{up}} \leq M.(1 - q_{ij}^{It_{up}}) + (\dfrac{r_{ij}.H_{ij}^{It_{up}} + x_{ij}.G_{ij}^{It_{up}}}{U_0}) \\ \qquad , It_{up} = 1,2,... \\ U_i^{It_{up}} - U_j^{It_{up}} \geq -M.(1 - q_{ij}^{It_{up}}) + (\dfrac{r_{ij}.H_{ij}^{It_{up}} + x_{ij}.G_{ij}^{It_{up}}}{U_0}) \end{cases} \tag{30}$$

$$\begin{cases} -S_{ij}^{\max}.q_{ij}^{It_{up}} \leq H_{ij}^{It_{up}} \leq S_{ij}^{\max}.q_{ij}^{It_{up}} \\ \qquad , It_{up} = 1,2,... \\ -S_{ij}^{\max}.q_{ij}^{It_{up}} \leq G_{ij}^{It_{up}} \leq S_{ij}^{\max}.q_{ij}^{It_{up}} \end{cases} \tag{31}$$

$$\begin{cases} 0 \leq P_{shed,j}^{It_{up}} \leq P_{L.j} \\ \qquad , It_{up} = 1,2,... \\ 0 \leq Q_{shed,j}^{It_{up}} \leq Q_{L.j} \end{cases} \tag{32}$$

$$\begin{cases} P_{DG,j}^{\min} \le P_{DG,j}^{It_{up}} \le P_{DG,j}^{\max} \\ \\ Q_{DG,j}^{\min} \le Q_{DG,j}^{It_{up}} \le Q_{DG,j}^{\max} \end{cases} \quad , It_{up} = 1,2,... \tag{33}$$

$$U_j^{\min} \le U_j^{It_{up}} \le U_j^{\max} \quad , It_{up} = 1,2,... \tag{34}$$

Topology constraints:

$$\sum_{ij \in L} q_{ij}^{It_{up}} = N_{bus} - \sum_{j \in N} \gamma'^{It_{up}}_j \quad , It_{up} = 1,2,... \tag{35}$$

$$\begin{cases} \sum_{s \in \omega(j)} F_{js}^{It_{up}} - \sum_{i \in \theta(j)} F_{ij}^{It_{up}} \ge -1 - M.\gamma'^{It_{up}}_j .Groot_j - M.\psi_j^{It_{up}} \\ \\ \sum_{s \in \omega(j)} F_{js}^{It_{up}} - \sum_{i \in \theta(j)} F_{ij}^{It_{up}} \le -1 + M.\gamma'^{It_{up}}_j .Groot_j + M.\psi_j^{It_{up}} \end{cases} \quad , It_{up} = 1,2,... \tag{36}$$

$$\begin{cases} qq_{ij}^{It_{up}} \ge z_{ij} \\ qq_{ij}^{It_{up}} \ge \hat{v}_{ij}^{It_{up}} \\ qq_{ij}^{It_{up}} \le z_{ij} + \hat{v}_{ij}^{It_{up}} \end{cases} \quad \begin{cases} q_{ij}^{It_{up}} \le qq_{ij}^{It_{up}} \\ q_{ij}^{It_{up}} \le w'^{It_{up}}_{ij} \\ q_{ij}^{It_{up}} \ge qq_{ij}^{It_{up}} + w'^{It_{up}}_{ij} - 1 \end{cases} \quad , It_{up} = 1,2,... \tag{37}$$

$$\begin{cases} \varphi_j^{It_{up}} \le \sum_{s \in \omega(j)} (1 - qq_{js}^{It_{up}}) + \sum_{i \in \theta(j)} (1 - qq_{ij}^{It_{up}}) \\ \\ \varphi_j^{It_{up}} \ge \sum_{s \in \omega(j)} (1 - qq_{js}^{It_{up}}) / M + \sum_{i \in \theta(j)} (1 - qq_{ij}^{It_{up}}) / M \end{cases} \quad , It_{up} = 1,2,... \tag{38}$$

$$\begin{cases} \psi_j^{It_{up}} \le \gamma'^{It_{up}}_j \\ \psi_j^{It_{up}} \le \varphi_j^{It_{up}} \\ \psi_j^{It_{up}} \ge \varphi_j^{It_{up}} + \gamma'^{It_{up}}_j - 1 \end{cases} \quad , It_{up} = 1,2,... \tag{39}$$

It_{up} is the UP iteration index.

Lower level problem – Master problem (Level 2)

When level 1 was solved and hardening plans were identified, the lower level is converted as follows:

$$\max_{v \in L} \min_{w \in L, \gamma \in N} \min_{\{P_{sehd,j}, Q_{shed,j}, P_{DG}, Q_{DG}, H, G, U, F\}} \sum_{j \in N} P_{shed,j} \quad (40)$$

In this section we have two-level problems. The L-MP determines the optimal attack plans and the optimal restoration plans will be obtained in the L-SP. Lower level problem-Master problem (L-MP):

$$\max_{v \in L} \min_{\{P_{sehd,j}, Q_{shed,j}, P_{DG}, Q_{DG}, H, G, U, F\}} \sum_{j \in N} P_{shed,j} \quad (41)$$

$\sum_{j \in N} P_{shed,j}$ is a LP and we can change to its dual form [19,20], so:

$$\max_{v \in L} \max_{\{\eta_1 - \eta_{16}\}} f(\eta) \quad (42)$$

Where η_1 - η_{16} is the dual variable to P_{shed}, Q_{shed}, P_{DG}, Q_{DG}, H, G, U, and f(η) is the dual objective function. η_1, η_2 are the dual variable for Eq. (6), η_3, η_4 for Eq. (7), η_5, η_6, η_7, η_8 for Eq. (8), η_9,η_{10} for Eq. (9), η_{11}, η_{12}, η_{13}, η_{14} for Eq. (10) and η_{15}, η_{16} for Eq. (11).

The general formulation of level 2:

$$\text{OF: } \max \beta \quad (43)$$

Constraints:

$$\sum_{ij \in L} (1 - v_{ij}) \le B_a \quad (44)$$

$$\begin{aligned}\beta \le & -\sum_{j \in N} P_{L,j}.\eta_{1,j}^{It_{lp}} - \sum_{j \in N} Q_{L,j}.\eta_{2,j}^{It_{lp}} + \sum_{ij \in N} M.(1-q_{ij}).\eta_{3,ij}^{It_{lp}} + \sum_{ij \in N} M.(1-q_{ij}).\eta_{4,ij}^{It_{lp}} \\ & + \sum_{ij \in L} S_{ij}^{\max}.q_{ij}.\eta_{5,ij}^{It_{lp}} + \sum_{ij \in L} S_{ij}^{\max}.q_{ij}.\eta_{6,ij}^{It_{lp}} + \sum_{ij \in L} M.(1-q_{ij}).\eta_{7,ij}^{It_{lp}} + \sum_{ij \in L} M.(1-q_{ij}).\eta_{8,ij}^{It_{lp}} \\ & + \sum_{j \in N} P_{L,j}.\eta_{9,j}^{It_{lp}} + \sum_{j \in N} Q_{L,j}.\eta_{10,j}^{It_{lp}} - \sum_{j \in N} P_{DG,\min,j}.\eta_{11,j}^{It_{lp}} + \sum_{j \in N} P_{DG,\max,j}.\eta_{12,j}^{It_{lp}} \\ & - \sum_{j \in N} Q_{DG,\min,j}.\eta_{13,j}^{It_{lp}} + \sum_{j \in N} Q_{DG,\max,j}.\eta_{14,j}^{It_{lp}} - \sum_{j \in N} U_{\min,j}.\eta_{15,j}^{It_{lp}} + \sum_{j \in N} U_{\max,j}.\eta_{16,j}^{It_{lp}}\end{aligned} \quad (45)$$

$$-\eta_{1,j}^{It_{lp}} + \eta_{9,j}^{It_{lp}} \le 1 \qquad , It_{lp} = 1,2,... \quad (46)$$

$$-\eta_{2,j}^{It_{lp}} + \eta_{10,j}^{It_{lp}} \le 0 \qquad , It_{lp} = 1,2,... \quad (47)$$

$$-\eta_{1,j}^{It_{lp}} - \eta_{11,j}^{It_{lp}} + \eta_{12,j}^{It_{lp}} \le 0 \qquad , It_{lp} = 1,2,... \quad (48)$$

$$-\eta_{2,j}^{It_{lp}} - \eta_{13,j}^{It_{lp}} + \eta_{14,j}^{It_{lp}} \le 0 \qquad , It_{lp} = 1,2,... \quad (49)$$

$$\eta_{1,i}^{It_{lp}} - \eta_{1,j}^{It_{lp}} - \left(\frac{r_{ij}}{U_0}\right).\eta_{3,ij}^{It_{lp}} + \left(\frac{r_{ij}}{U_0}\right).\eta_{4,ij}^{It_{lp}} - \eta_{5,ij}^{It_{lp}} + \eta_{6,ij}^{It_{lp}} = 0 \qquad ,It_{lp} = 1,2,... \tag{50}$$

$$\eta_{2,i}^{It_{lp}} - \eta_{2,j}^{It_{lp}} - \left(\frac{x_{ij}}{U_0}\right).\eta_{3,ij}^{It_{lp}} + \left(\frac{x_{ij}}{U_0}\right).\eta_{4,ij}^{It_{lp}} - \eta_{7,ij}^{It_{lp}} + \eta_{8,ij}^{It_{lp}} = 0 \qquad ,It_{lp} = 1,2,... \tag{51}$$

$$\sum_{s\in\omega(j)} \eta_{3,js}^{It_{lp}} - \sum_{i\in\theta(j)} \eta_{3,ij}^{It_{lp}} - \sum_{s\in\omega(j)} \eta_{4,js}^{It_{lp}} + \sum_{i\in\theta(j)} \eta_{4,ij}^{It_{lp}} - \eta_{15,j}^{It_{lp}} + \eta_{16,j}^{It_{lp}} = 0 \qquad ,It_{lp} = 1,2,... \tag{52}$$

$$\eta_3^{It_{lp}} \le 0, \eta_4^{It_{lp}} \ge 0, \eta_5^{It_{lp}} \ge 0, \eta_6^{It_{lp}} \le 0, \eta_7^{It_{lp}} \ge 0, \eta_8^{It_{lp}} \le 0, \eta_9^{It_{lp}} \le 0, \eta_{10}^{It_{lp}} \le 0$$
$$, \eta_{11}^{It_{lp}} \ge 0, \eta_{12}^{It_{lp}} \le 0, \eta_{13}^{It_{lp}} \ge 0, \eta_{14}^{It_{lp}} \le 0, \eta_{15}^{It_{lp}} \ge 0, \eta_{16}^{It_{lp}} \le 0 \qquad ,It_{lp} = 1,2,... \tag{53}$$

$$\begin{cases} qq_{ij}^{It_{lp}} \ge \hat{z}_{ij} \\ qq_{ij}^{It_{lp}} \ge v_{ij} \\ qq_{ij}^{It_{lp}} \le \hat{z}_{ij} + v_{ij} \end{cases} \qquad \begin{cases} q_{ij}^{It_{lp}} \le qq_{ij}^{It_{lp}} \\ q_{ij}^{It_{lp}} \le w_{ij}'^{It_{lp}} \\ q_{ij}^{It_{lp}} \ge qq_{ij}^{It_{lp}} + w_{ij}'^{It_{lp}} - 1 \end{cases} \qquad ,t = 1,2,... \tag{54}$$

It_{lp} is the LP iteration index. η_3 and η_4, η_5 and η_6, η_7 and η_8 are the nonlinear parts of Eq.(45). We can linearize these parts with this form:
$\sum_{ij\in L} M.(1-q_{ij}).\eta_{3,ij}^{It_{lp}} + \sum_{ij\in L} M.(1-q_{ij}).\eta_{4,ij}^{It_{lp}}$ and for simplicity $\mu_1 = M.(1-q).(\eta_3+\eta_4)$.

The variable μ can be linearized by the following functions:

$$\begin{cases} \mu_1 \le 0 \\ \mu_1 \ge -M'.(1-q) \\ \mu_1 \le M.(\eta_3+\eta_4) + M'.q \\ \mu_1 \ge M.(\eta_3+\eta_4) - M'.q \end{cases} \tag{55}$$

In the above functions M and M' are large numbers to linearize the non-linear terms in the constraints. The other variables (η_5 and η_6, η_7 and η_8) have linearized by this method [25].

Lower level problem – Sub problem (Level 3)

The aim of this level is to find the optimal islanding and reconfiguration plans which keep the minimum load shedding.

The general formulation of level 3:

Objective: $$\min \quad \sum_{j\in N} P_{shed,j} \tag{56}$$

$$\{\gamma, w, P_{sehd,j}, Q_{shed,j}, P_{DG}, Q_{DG}, H, G, U, F\}$$

Constraints: Eq. (5) – Eq. (11), Eq. (14), Eq. (15), Eq. (20) – Eq. (23)

The all problems are mixed-integer linear problem. A flowchart of the suggested algorithm is shown in Fig. 1.

Second Model (tri-level of hardening, attack and optimal placement of DGs)

In the second model, we assume a three-level model, the only difference with the first model is in its third level. Indeed in this model, we find the optimal DG placement in the third level (instead of finding optimal reconfiguration of first model). In other words, in this model, the location of DGs is not known from the beginning to the end of the algorithm is to determine the optimal placement of DGs and their production rate. In this model, as in the first model, we consider three levels. The first level is the level of reinforcement, level 2 is the level of attack and failure, and in the third level, optimal placement and the size of DGs is determined. The formulation of this model is as follows.

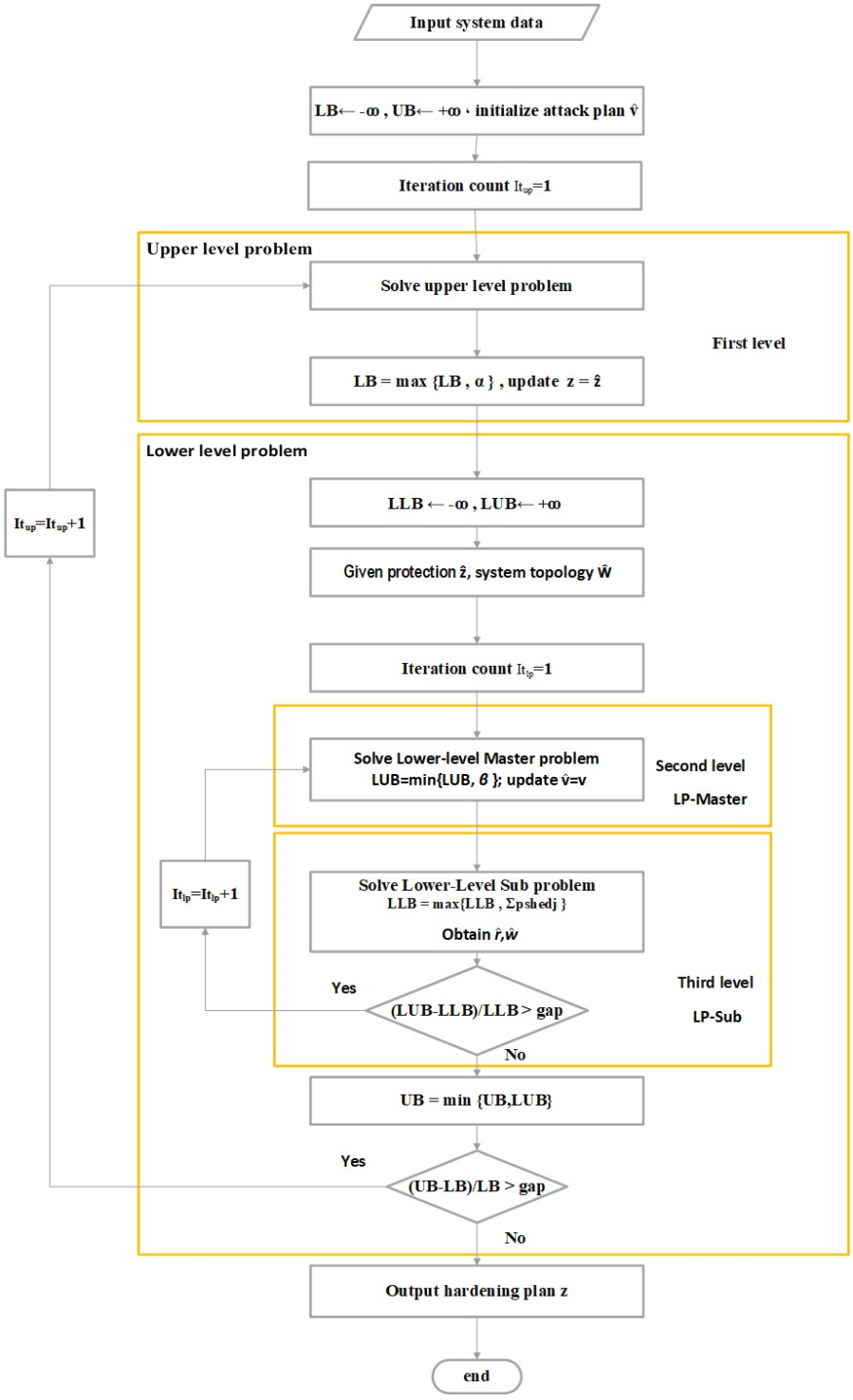

Fig 1. Implementation flowchart of first model

Lower level problem – Sub problem (level 3)

In this model, we consider DG_j as a integer variable for determining which bus to install DGs. Indeed if DG_j =1 means that DG in bus j has been installed.

Objective function: $\min \sum_{j\in N} P_{shed,j}$ (57)

$$\left\{\gamma, DG_j, P_{sehd,j}, Q_{shed,j}, P_{DG}, Q_{DG}, H, G, U, F\right\}$$

Operational constraints:

$$\sum_{j\in N} DG_j \le GDG \tag{58}$$

$$\begin{cases} P_{DG,j}^{It_{lp}} - (P_{L,j} - P_{shed,j}^{It_{lp}}) = \sum_{s\in\omega(j)} H_{js}^{It_{lp}} - \sum_{i\in\theta(j)} H_{ij}^{It_{lp}} \\ \\ Q_{DG,j}^{It_{lp}} - (Q_{L,j} - Q_{shed,j}^{It_{lp}}) = \sum_{s\in\omega(j)} G_{js}^{It_{lp}} - \sum_{i\in\theta(j)} G_{ij}^{It_{lp}} \end{cases} \quad , It_{lp} = 1,2,... \tag{59}$$

$$\begin{cases} U_i^{It_{lp}} - U_j^{It_{lp}} \le M.(1-q_{ij}^{It_{lp}}) + (\dfrac{r_{ij}.H_{ij}^{It_{lp}} + x_{ij}.G_{ij}^{It_{lp}}}{U_0}) \\ \\ U_i^{It_{lp}} - U_j^{It_{lp}} \ge -M.(1-q_{ij}^{It_{lp}}) + (\dfrac{r_{ij}.H_{ij}^{It_{lp}} + x_{ij}.G_{ij}^{It_{lp}}}{U_0}) \end{cases} \quad , It_{lp} = 1,2,... \tag{60}$$

$$\begin{cases} -S_{ij}^{\max}.q_{ij}^{It_{lp}} \le H_{ij}^{It_{lp}} \le S_{ij}^{\max}.q_{ij}^{It_{lp}} \\ \\ -S_{ij}^{\max}.q_{ij}^{It_{lp}} \le G_{ij}^{It_{lp}} \le S_{ij}^{\max}.q_{ij}^{It_{lp}} \end{cases} \quad , It_{lp} = 1,2,... \tag{61}$$

$$\begin{cases} 0 \le P_{shed,j}^{It_{lp}} \le P_{L.j} \\ \\ 0 \le Q_{shed,j}^{It_{lp}} \le Q_{L.j} \end{cases} \quad , It_{lp} = 1,2,... \tag{62}$$

$$\begin{cases} P_{DG,j}^{\min} * DG_j \le P_{DG,j}^{It_{lp}} \le P_{DG,j}^{\max} * DG_j \\ \\ Q_{DG,j}^{\min} * DG_j \le Q_{DG,j}^{It_{lp}} \le Q_{DG,j}^{\max} * DG_j \end{cases} \quad , It_{lp} = 1,2,... \tag{63}$$

$$U_j^{\min} \le U_j^{It_{lp}} \le U_j^{\max} \quad , It_{lp} = 1,2,... \tag{64}$$

Topology constraints:

$$\sum_{ij\in L} q_{ij}^{It_{lp}} = N_{bus} - \sum_{j\in N} \gamma_j^{It_{lp}} \qquad ,It_{lp} = 1,2,... \tag{65}$$

$$\begin{cases} \sum_{s\in\omega(j)} F_{js}^{It_{lp}} - \sum_{i\in\theta(j)} F_{ij}^{It_{lp}} \geq -1 - M.\gamma_j^{It_{lp}}.Groot_j - M.y_j^{It_{lp}} \\ \qquad\qquad ,It_{lp} = 1,2,... \\ \sum_{s\in\omega(j)} F_{js}^{It_{lp}} - \sum_{i\in\theta(j)} F_{ij}^{It_{lp}} \leq -1 + M.\gamma_j^{It_{lp}}.Groot_j + M.y_j^{It_{lp}} \end{cases} \tag{66}$$

$$\begin{cases} qq_{ij}^{It_{lp}} \geq z_{ij} \\ qq_{ij}^{It_{lp}} \geq \hat{v}_{ij}^{It_{lp}} \qquad ,It_{lp} = 1,2,... \\ qq_{ij}^{It_{lp}} \leq z_{ij} + \hat{v}_{ij}^{It_{lp}} \end{cases} \tag{67}$$

$$\begin{cases} \varphi_j^{It_{lp}} \leq \sum_{s\in\omega(j)} (1 - qq_{js}^{It_{lp}}) + \sum_{i\in\theta(j)} (1 - qq_{ij}^{It_{lp}}) \\ \qquad\qquad ,It_{lp} = 1,2,... \\ \varphi_j^{It_{lp}} \geq \sum_{s\in\omega(j)} (1 - qq_{js}^{It_{lp}})/M + \sum_{i\in\theta(j)} (1 - qq_{ij}^{It_{lp}})/M \end{cases} \tag{68}$$

$$\begin{cases} \psi_j^{It_{lp}} \leq \gamma_j^{It_{lp}} \\ \psi_j^{It_{lp}} \leq \varphi_j^{It_{lp}} \qquad ,It_{lp} = 1,2,... \\ \psi_j^{It_{lp}} \geq \varphi_j^{It_{lp}} + \gamma_j^{It_{lp}} - 1 \end{cases} \tag{69}$$

It_{lp} is the LP iteration index. The all problems are mixed-integer linear problem. A flowchart of the suggested algorithm is shown in Fig. 2.

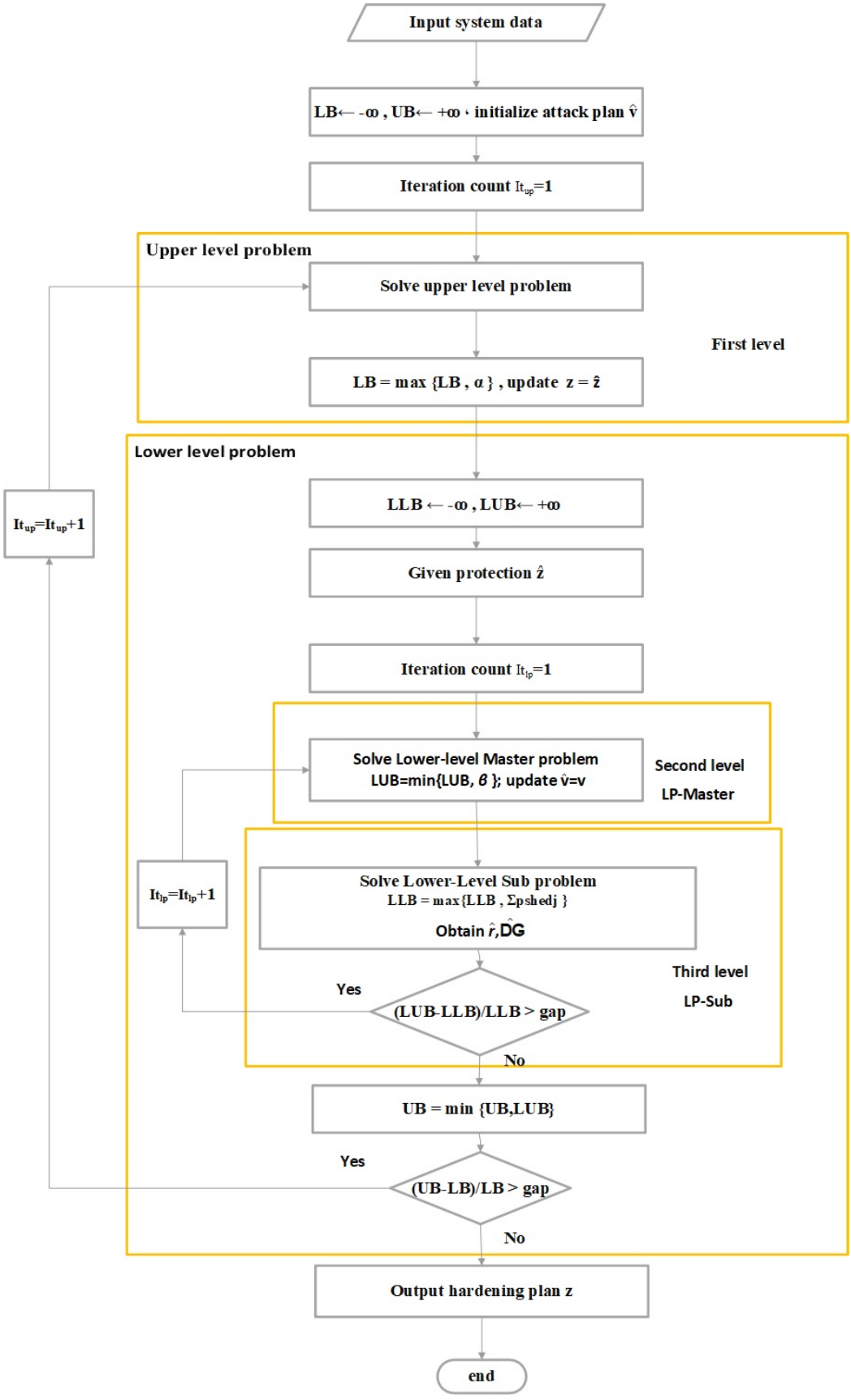

Fig 2. Implementation flowchart of second model

4. Case study

Here, an IEEE-33 bus test system has been selected to confirm the efficiency of the suggested models. The all data of this test system have given in table 3 [26]. The form of this test system is exhibited on Fig. 3.

Table 3. The all data of the IEEE-33 bus test system

	Parameter type	Value
Cap	Capacity of DGs	5 MVA
	Capacity of branches	0.5 MVA
Net	Base voltage	12.66 kV
	power base	100 MVA
Range	Voltage magnitude range	[0.9 , 1.1] p.u
	lower and upper limits of active power of DGS	[0.06,0.6] MW
	lower and upper limits of reactive power of DGS	[0.05,0.5] MVAR
Other parameter	MIP gap	0.1% other parameters
	The total load	3.71MW+ 2.30MVar

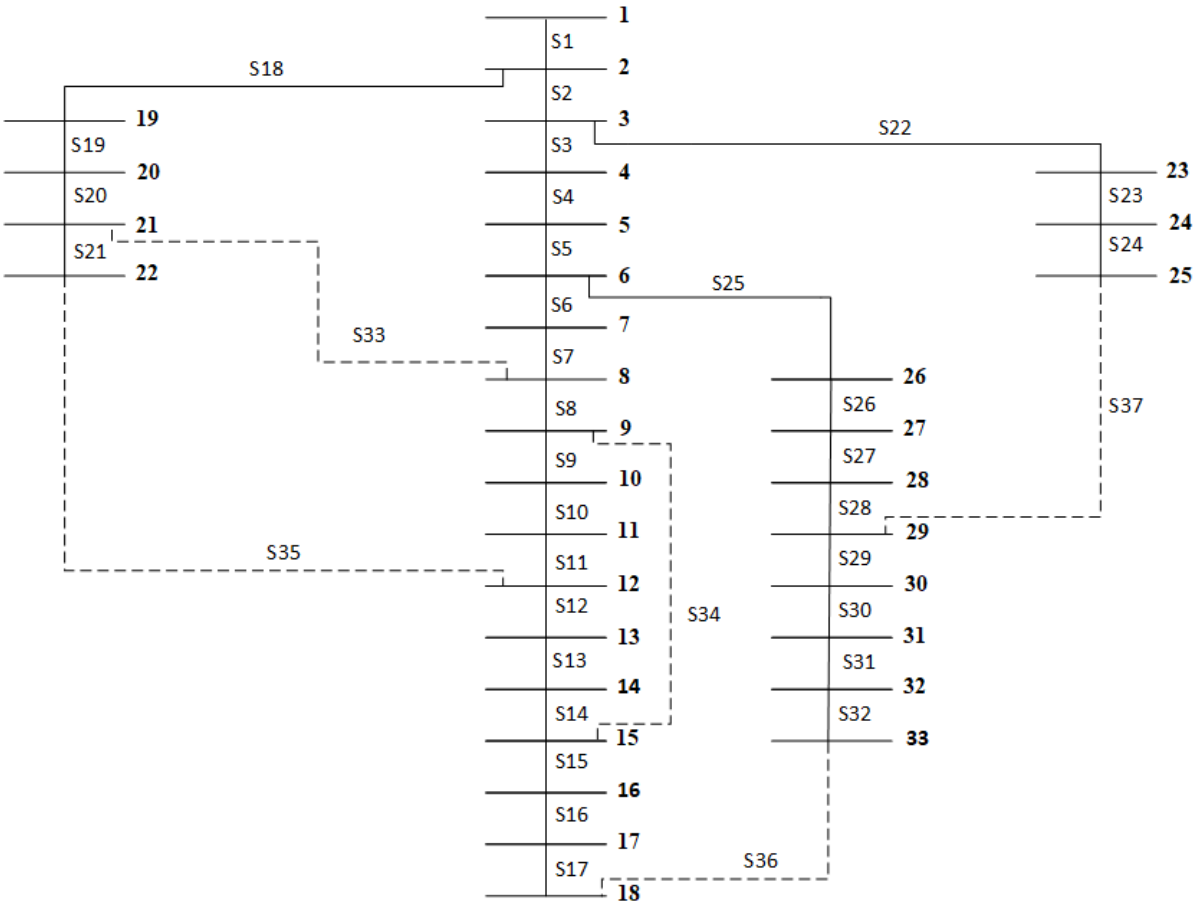

Fig 3. A modified IEEE 33-bus test system

Computational results:

In this section, the modeling and input information which references in part 3 are implemented and simulated in the software, and the results are presented in the form of diagrams and tables.

A) First Model (tri-level of hardening, attack and optimal reconfiguration programs)

In this section, the simulation results of the first model are presented. In this model, 5 different attack scenarios (B_a = 1 to B_a = 5) are considered to simulate attack scenarios. The proposed model is simulated in four different sections and their results are compared with each other.

A.1) non reconfigurable system – no hardening (B_h=0):

At this stage, the studied network is not able to be reconfigured and hardened and strengthened (B_h = 0). In this step, we consider 5 scenarios with different values of attack and different damage (B_a = 1 to B_a = 5). In fact, in this case 5 simulation implementation processes are performed with different amounts of attack and damage budget. Obviously, with increasing damage and lines outages in the network, the amount of load shedding increases accordingly. This is confirmed by simulation results.

In the first step, we examine the network with the probability of an attack and failure in only one line (B_a = 1). Obviously, the worst case scenario occurs when the line network interface of the studied network to the upper network (line number 1) is cut. In this case, feeding the buses is only possible from the distribution resources available in the network. The structural form of the network after the occurrence of this scenario and microgrid formation is shown in Fig. 4. The curtailed power in this scenario is 0.71 MW.

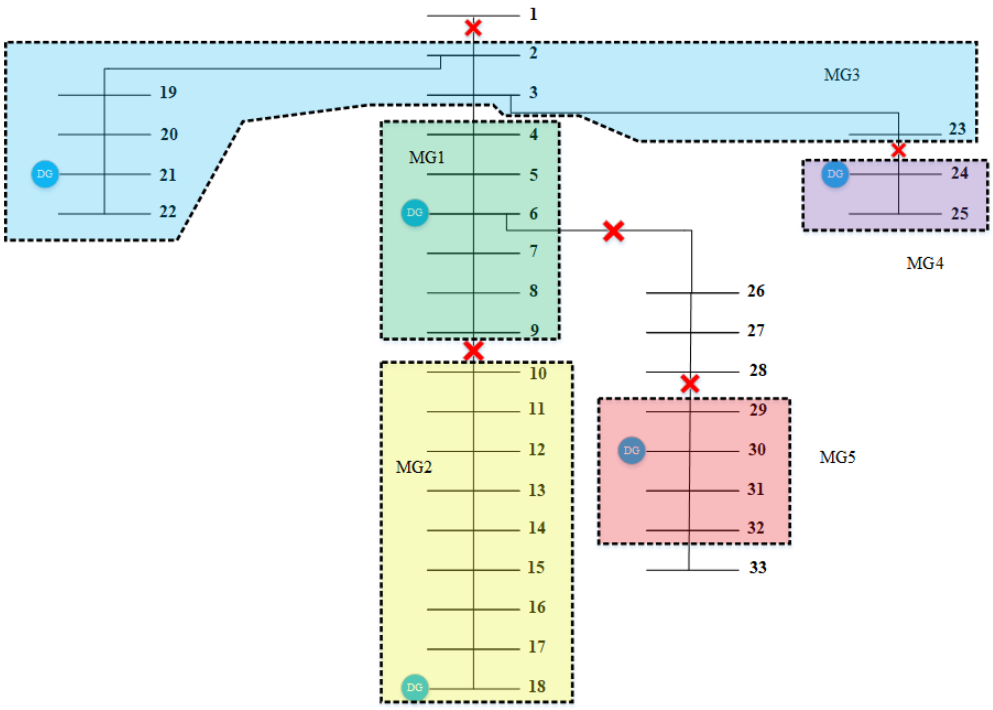

Fig. 4. Network structure after an attack in the non-reconfigurable and no-hardening network

The other lines have been cut in the figure are applied by the binary variable selecting / not selecting lines (W). With this scenario, 5 microgrids will form independently of each other. During the occurrence of this process, for a definite reason, the system can`t be powered from the above network, feeding the buses only through the available DGs in the network, so the load of some buses must be cut off. The schematic of the network is shown in Fig. 5 after obtaining the other scenarios.

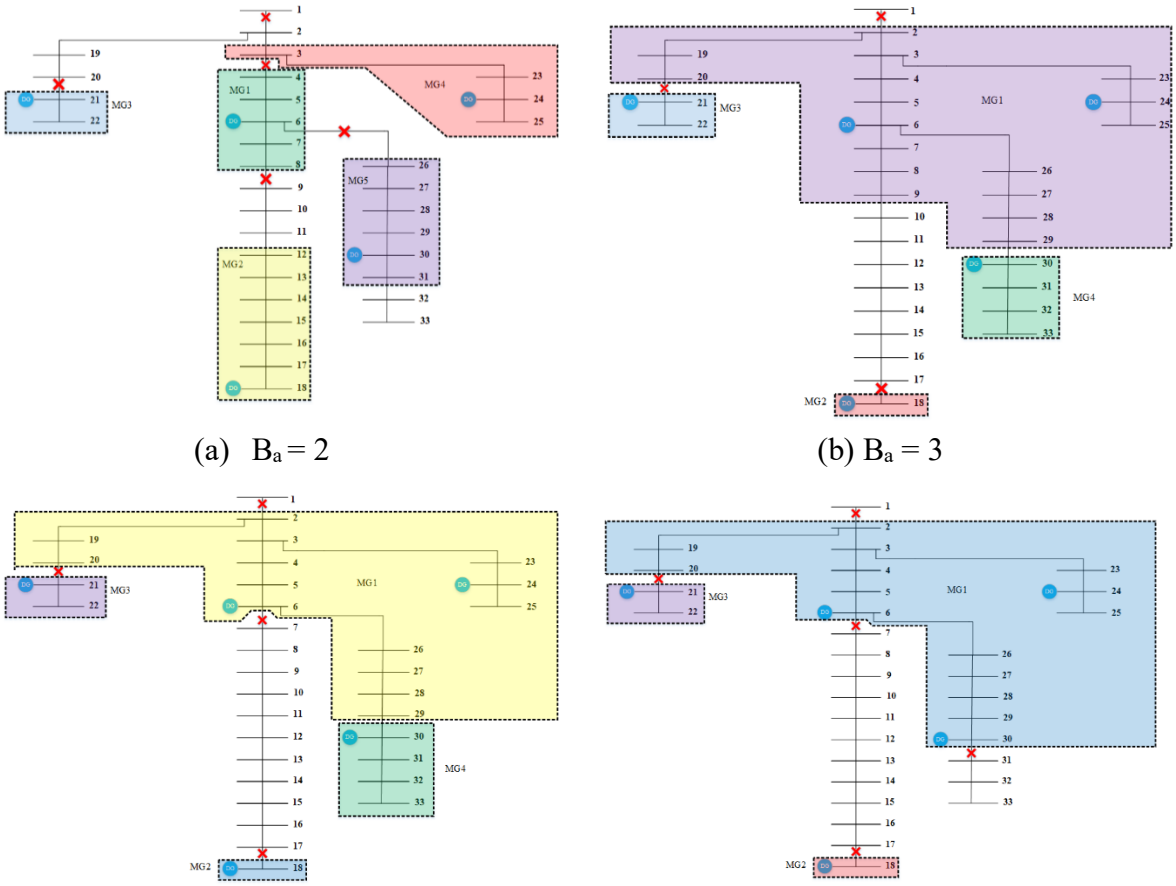

(a) $B_a = 2$ (b) $B_a = 3$

(c) $B_a = 4$ (d) $B_a = 5$

Fig. 5. Network status after different scenarios (A.1)

The general information of the network (the amount of load shedding and the amount of DG resources production) is given in Table 4.

Table 4. The DGs active power production and load shedding of 5 scenarios (A.1)

scenario	$P_{DG,1}$ [MW]	$P_{DG,2}$ [MW]	$P_{DG,3}$ [MW]	$P_{DG,4}$ [MW]	$P_{DG,5}$ [MW]	Load shedding [MW]
Ba=1	0.6	0.6	0.6	0.6	0.6	0.71
Ba=2	0.6	0.51	0.18	0.6	0.6	1.22
Ba=3	0.6	0.09	0.18	0.6	0.6	1.64
Ba=4	0.51	0.09	0.18	0.6	0.6	1.73
Ba=5	0.35	0.09	0.18	0.6	0.6	1.89

As can be seen from the simulation results, the load shedding increases when the simultaneous attacks on the lines increase. This is shown in Fig. 6.

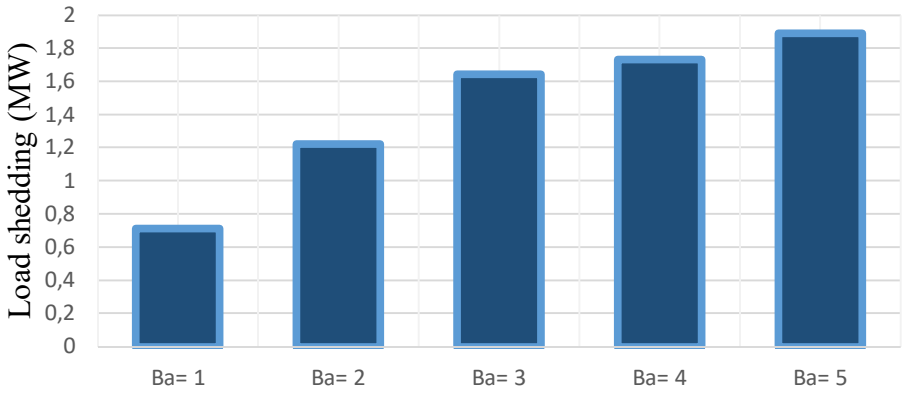

Fig .6. Comparison of load shedding with the increase in line faults in the network without reconfiguration and without hardening

A.2) reconfigurable system – no hardening (B_h=0):

At this stage, the studied network has the ability to be reconfigured but not hard and resistant (B_h = 0). Here, as in the previous step, we consider five scenarios with different attack budget. The following is a comparison between the effects of reconfiguration in reducing load shedding in similar scenarios. We consider the desired network by considering the occurrence of an attack (B_a=1). The simulation results confirm that disconnecting line 1, which is actually the system interface to the main network, is the worst possible situation. Fig. 7 shows the status of the network and the microgrids formation after this event.

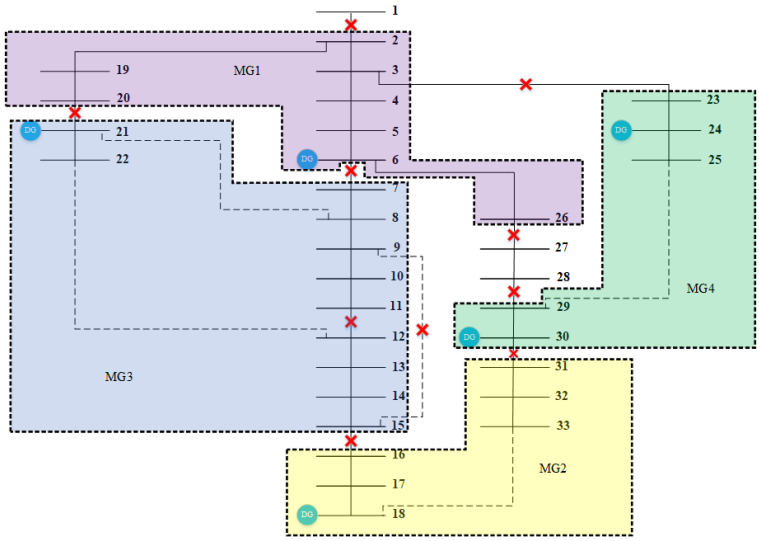

Fig. 7. Network structure with one attack and failure with reconfiguration and without hardening

The schematic of the network is shown in the Fig. 8 after obtaining the other scenarios.

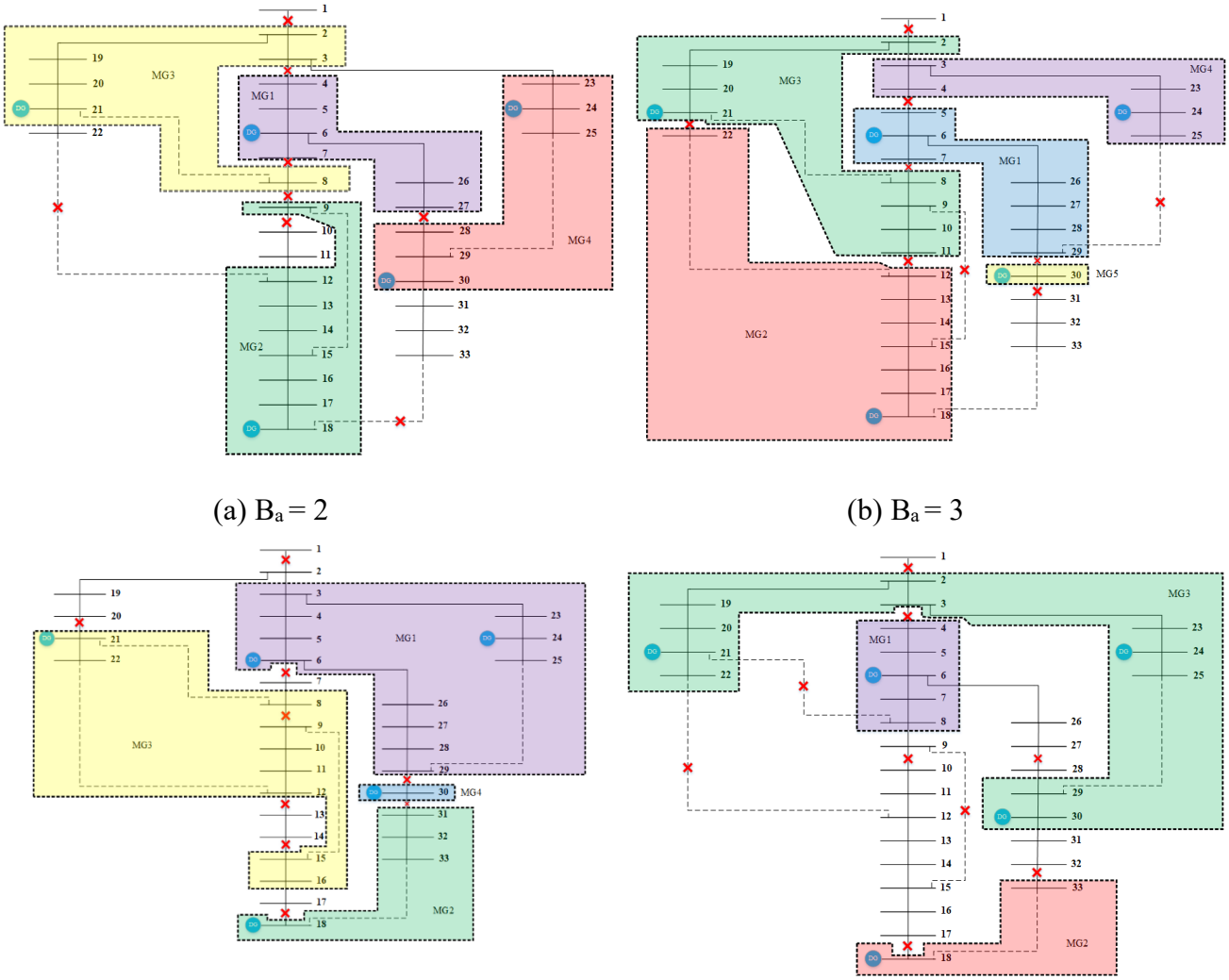

(a) $B_a = 2$ (b) $B_a = 3$

(c) $B_a = 4$ (d) $B_a = 5$

Fig. 8. Network status after different scenarios with reconfiguration (A.2)

The general network information in this section (reconfigurable network – no hardening) is given in Table 5.

Table 5. The DGs active power production and load shedding of 5 scenarios (A.2)

scenario	$P_{DG,1}$ [MW]	$P_{DG,2}$ [MW]	$P_{DG,3}$ [MW]	$P_{DG,4}$ [MW]	$P_{DG,5}$ [MW]	Load shedding [MW]
Ba=1	0.6	0.6	0.6	0.6	0.6	0.71
Ba=2	0.6	0.6	0.6	0.6	0.6	0.71
Ba=3	0.6	0.6	0.6	0.6	0.2	1.11
Ba=4	0.6	0.51	0.6	0.6	0.2	1.2
Ba=5	0.6	0.15	0.6	0.54	0.6	1.22

It can be seen that with the network reconfiguration capability, the load shedding is reduced. This is shown in Fig. 9.

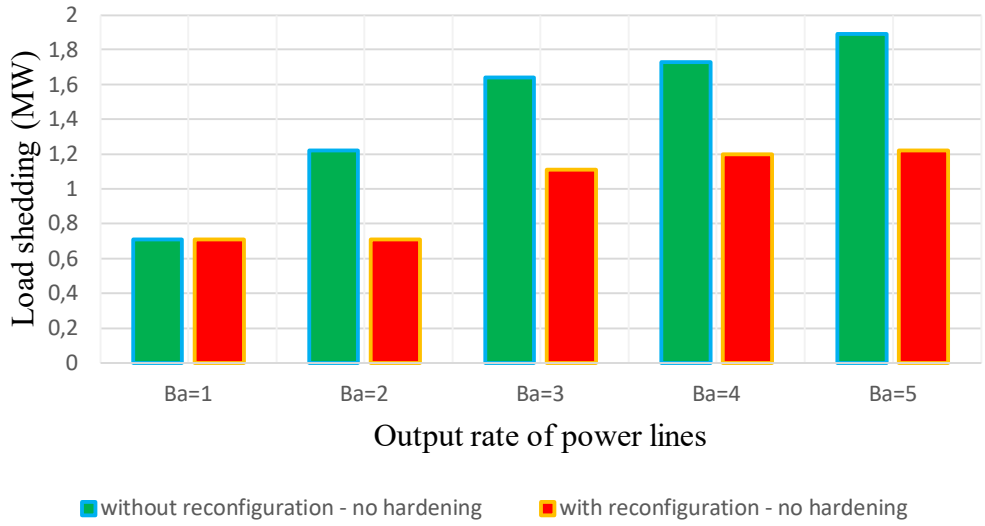

Fig. 9. Comparison of load shedding with the increase in line faults in the network without reconfiguration and no-hardening and the network with reconfiguration and no-hardening.

A.3) non reconfigurable system –hardening capability ($B_h \neq 0$):

In this section, we consider the studied network by considering the hardening and strength capability and without considering the reconfiguration. 5 scenarios with the number of different attack budget as well as the hardening budget of one line ($B_h = 1$) have been used in this section.

The system was studied by the occurrence of a failure and also considering the budget of strengthening the lines as much as one line, without considering the reconfiguration. According to the simulations, the cutting of line 1 has the greatest effect on the definite increase of the load and vice versa, the hardening of line 1 (as a result of which this line is not interrupted despite attack and failure) has the greatest effect on reducing the load shedding. Fig. 10 shows the schematic of the system, taking into account the above conditions. In this case, with the above processes, the cut-off electrical power is zero.

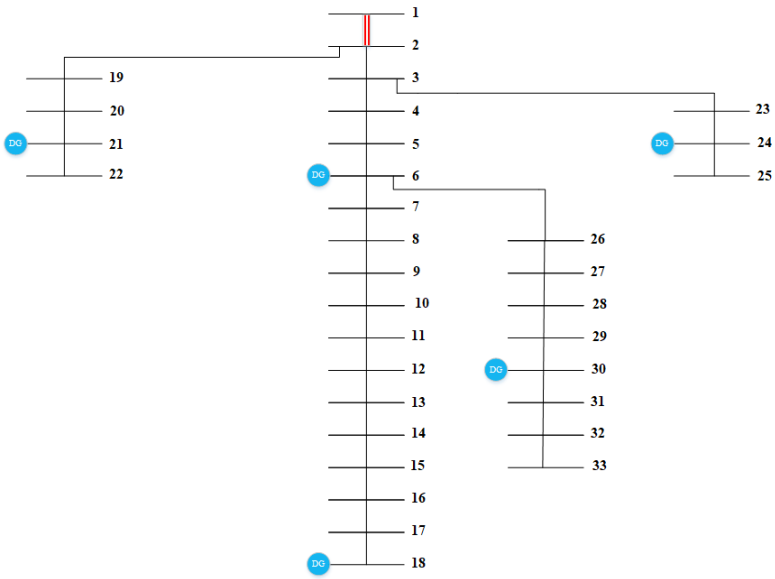

Fig. 10. Network status with an attack and one hardened line without reconfiguration.

The schematic of the network after occurring the other scenarios is shown in the fig. 11.

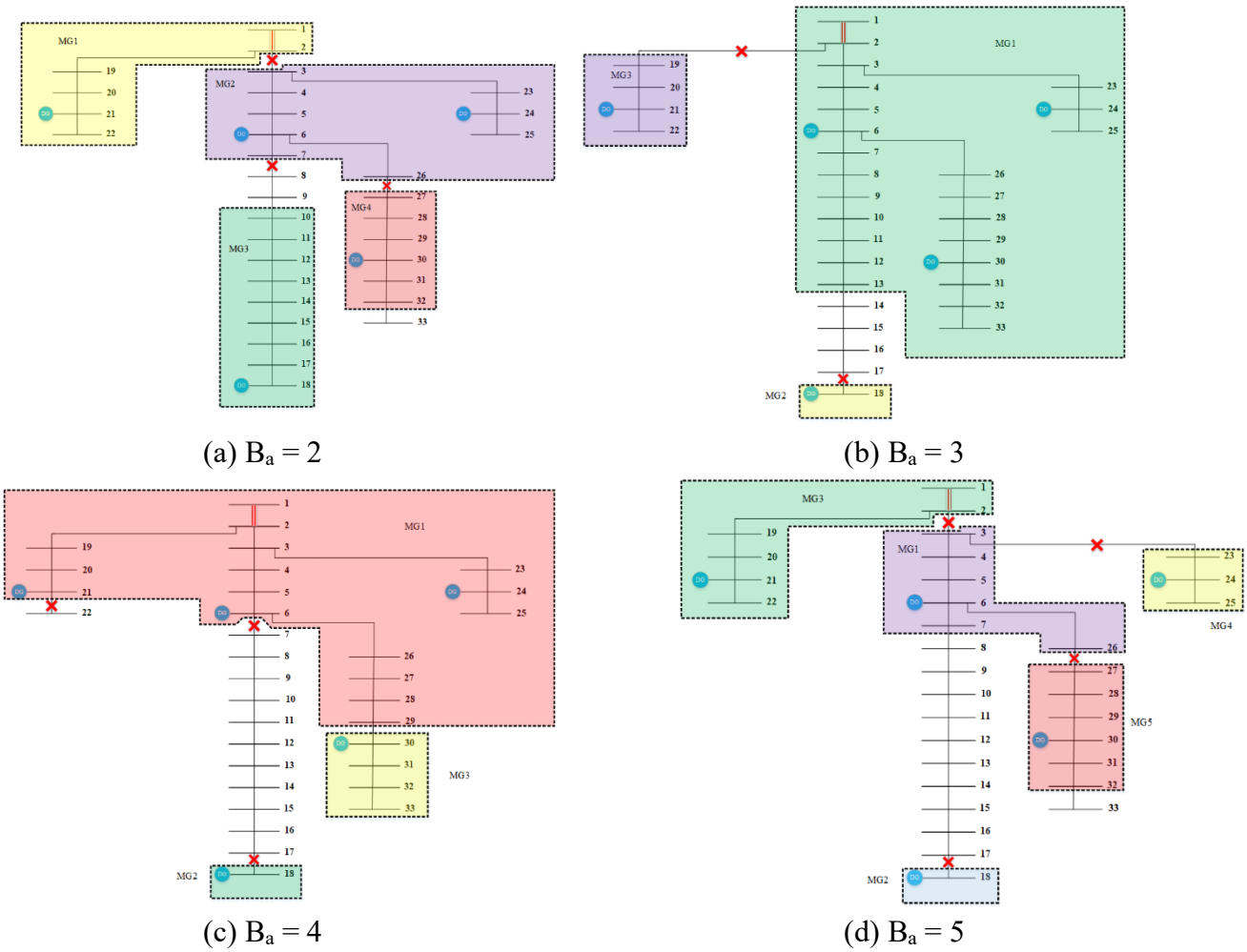

(a) $B_a = 2$ (b) $B_a = 3$

(c) $B_a = 4$ (d) $B_a = 5$

Fig. 11. Network status after different scenarios with hardening (A.3)

The following is a comparison of load shedding between scenarios similar to the no-hardening network and with the hardening capability as much as one line. There is also a comparison of the load shedding with the increase in the hardening budget. The general information of the network in this section (non-reconfigurable network hardening capability) is given in Table 6.

Table 6. The DGs active power production and load shedding of 5 scenarios (A.3)

scenario	$P_{DG,1}$ [MW]	$P_{DG,2}$ [MW]	$P_{DG,3}$ [MW]	$P_{DG,4}$ [MW]	$P_{DG,5}$ [MW]	$P_{upstream\ network}$ [MW]	Load shedding [MW]
Ba=1	0.6	0.6	0.6	0.6	0.6	0.71	0
Ba=2	0.6	0.6	0.1	0.6	0.6	0.36	0.85
Ba=3	0.6	0.09	0.36	0.6	0.6	0.57	0.89
Ba=4	0.44	0.09	0.09	0.6	0.6	0.71	1.18
Ba=5	0.6	0.09	0.09	0.6	0.6	0.37	1.36

According to the simulation results, it is clear that the load shedding has been reduced by hardening the network. This is shown in Fig. 12.

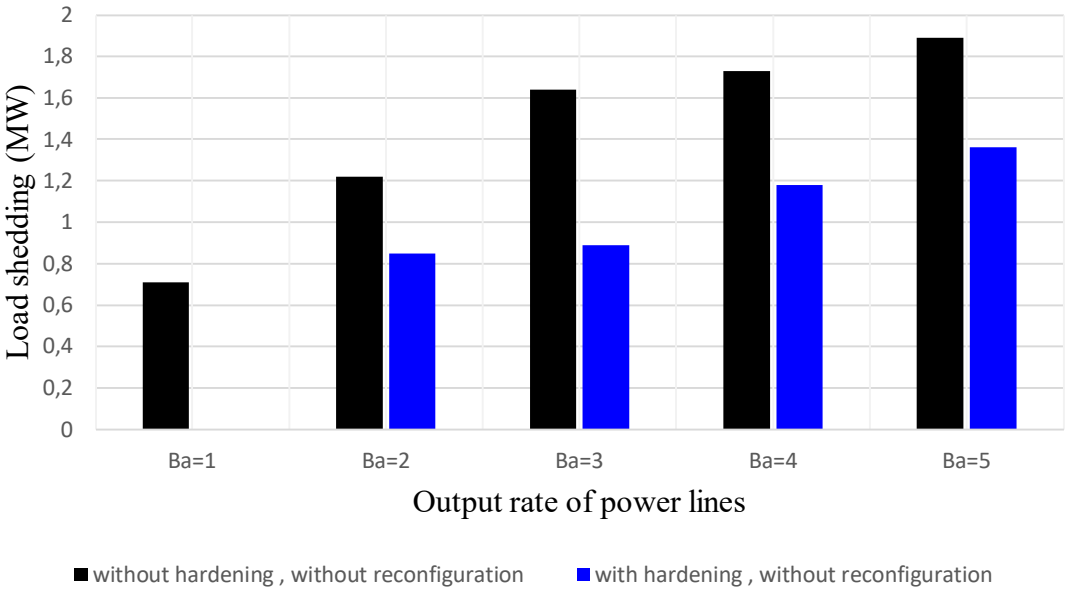

Fig. 12. Comparison of load shedding with the increase in line faults in the network without reconfiguration and no-hardening and the network with hardening and without reconfiguration.

Fig. 13 shows a comparison with different reinforcement budgets ($B_h = 0$, $B_h = 1$ and $B_h = 2$) for the study system. As it can be shown, by increasing of hardening budget, the load shedding is reduces.

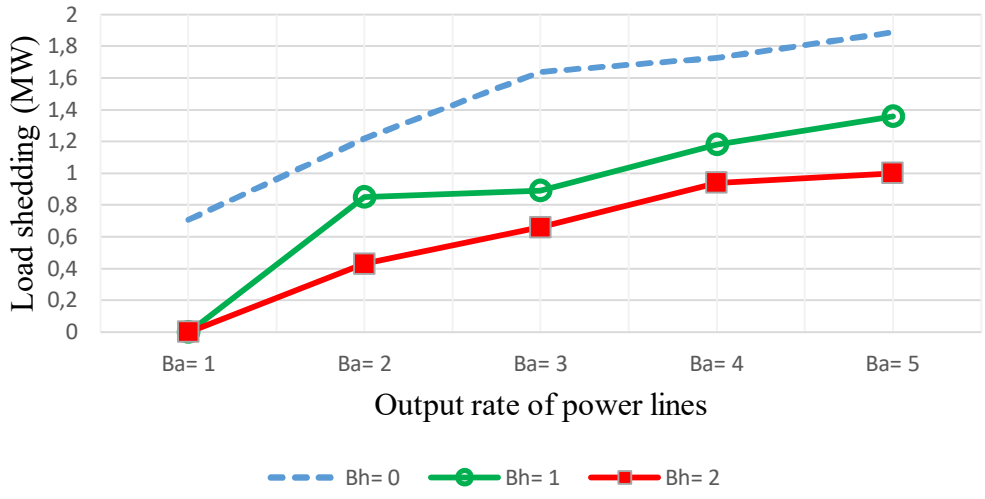

Fig. 13. Comparison of load shedding with three different hardening budgets

A.4) reconfigurable system –hardening capability ($B_h \neq 0$):

In the fourth step, we examine the simultaneous effect of hardening and reconfiguration on the grid to investigate changes in load shedding. As before, we consider 5 different attack scenarios with a line reinforcement budget ($B_h = 1$) in the presence of reconfiguration.

We simulated the system with an attack and a reinforcement budget (B_a=1 and B_h=1) in the presence of reconfiguration. According to Calculations, the output of line 1 has the greatest loss and the hardening of line 1 has the greatest advantage in terms of reduced cut-off power. The schematic of the system in this case is shown in Fig. 14.

The power cut off in this case is zero despite the attack on line 1 due to its hardening and strength, this line is not out of circuit and the system is still powered by the main grid. In fact, in this case, a large microgrid is formed, and also due to the power supply of the system from the upstream network, as well as the fact that the radial constraint is not violated, the tie lines related to the reconfiguration are cut off. The schematic of the network after occurring the other scenarios is shown in the fig. 15.

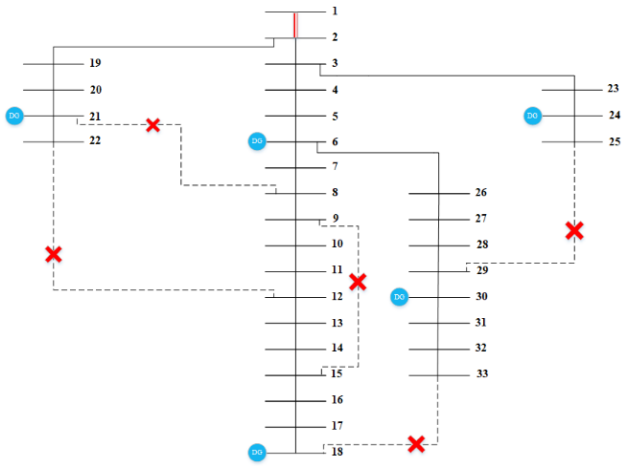

Fig. 14. Schematic of the system after a failure and a reinforcement program with reconfiguration

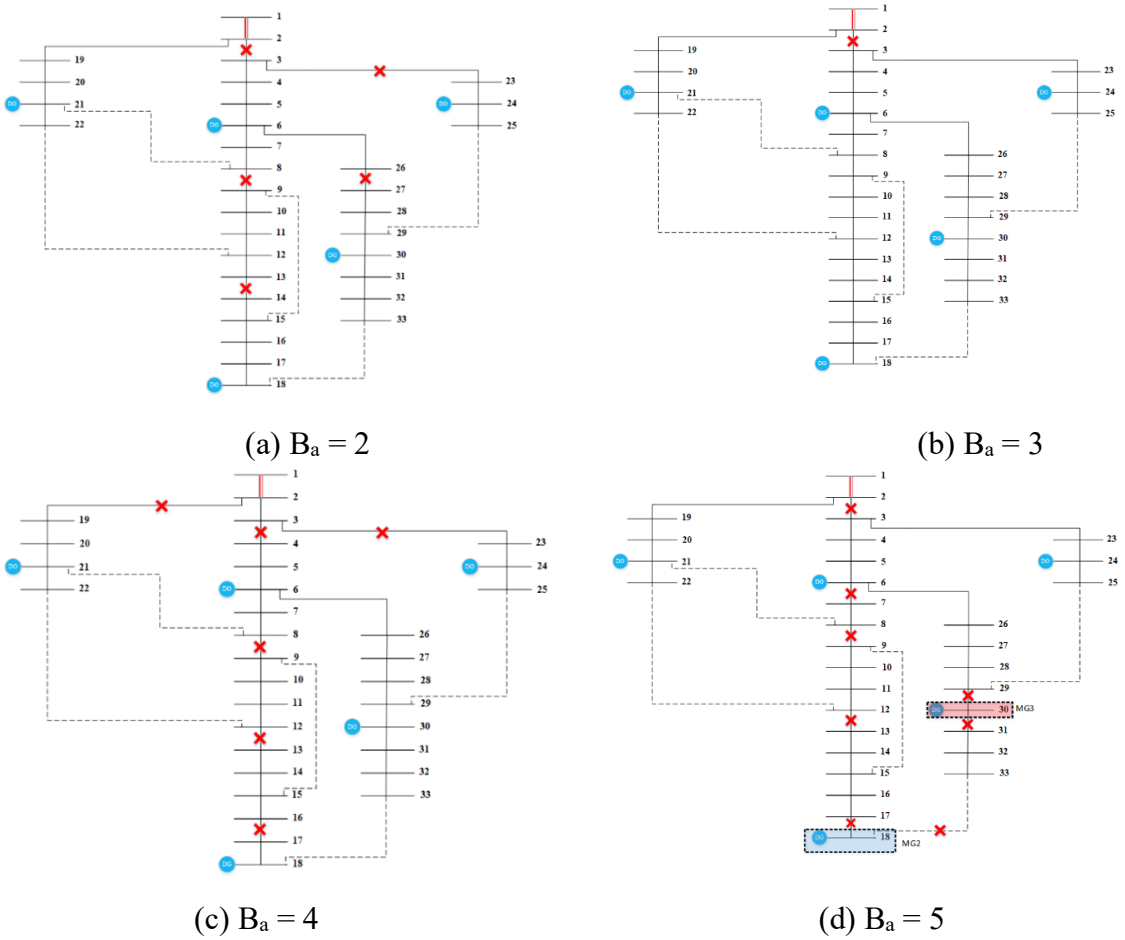

(a) $B_a = 2$ (b) $B_a = 3$

(c) $B_a = 4$ (d) $B_a = 5$

Fig. 15. Network status after different scenarios with hardening and reconfiguration (A.4).

The general information on the production of DGs and the amount of load shedding by reconfiguration-hardening state is provided in Table 7.

Table 7. The DGs active power production and load shedding of 5 scenarios (A.4)

scenario	$P_{DG,1}$ [MW]	$P_{DG,2}$ [MW]	$P_{DG,3}$ [MW]	$P_{DG,4}$ [MW]	$P_{DG,5}$ [MW]	$P_{upstream\ network}$ [MW]	Load shedding [MW]
Ba=1	0.6	0.6	0.6	0.6	0.6	0.71	0
Ba=2	0.6	0.6	0.6	0.6	0.6	0.71	0
Ba=3	0.56	0.15	0.6	0.6	0.6	0.78	0.42
Ba=4	0.6	0.6	0.6	0.42	0.6	0.28	0.61
Ba=5	0.6	0.09	0.6	0.6	0.2	0.71	0.91

A general comparison of all 4 states is given in Fig. 16. As can be seen, the last state is the most effectiveness for load shedding reduction.

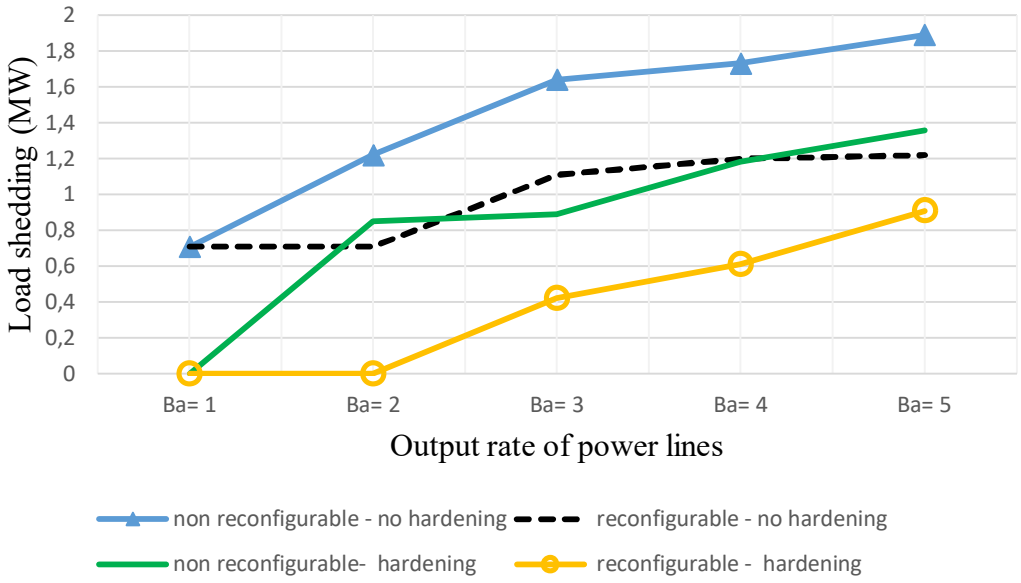

Fig. 16. Comparison of load shedding for 4 different modes in 5 scenarios.

B) Second model:

In the second model, we simulated the studied network by considering the optimal placement of DGs without reconfiguration. At this model, we have considered a three-level model, the difference between this and the previous model is that in the third level, instead of reconfiguration, we determine the optimal location of distribution resources. As in the first model, we consider 5 different attack scenarios and examine the network structure after these attacks occur. Assume the system to occur an attack (B_a=1). According to the simulation results, the output of line 1, has the greatest effect on increasing the load shedding. After this process occurs, the algorithm calculates the most optimal possible solution, as a result of which the optimal location of DGs is buses 2, 4, 5, 18 and 31, respectively. Fig. 17 shows the network structure after this mode. All DGs are in maximum production, and the load shedding in this scenario is 0.71 MW.

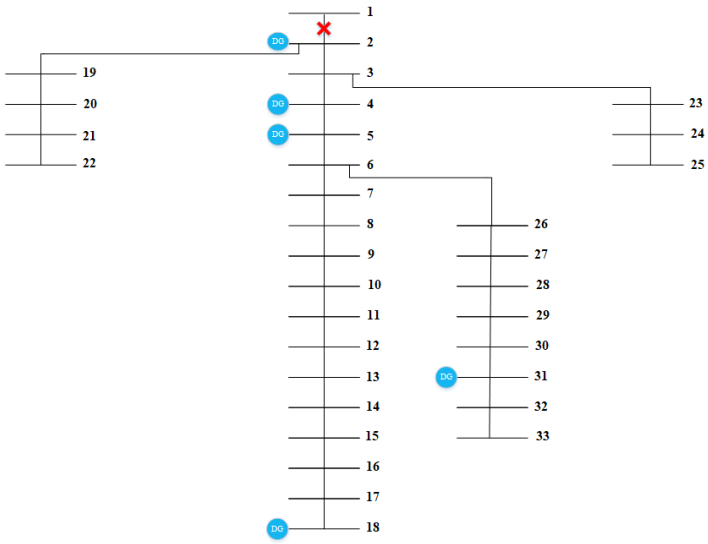

Fig. 17. The network structure after an attack

The status of the network and optimal DG placement after the occurrence of other scenarios is shown in Fig. 18.

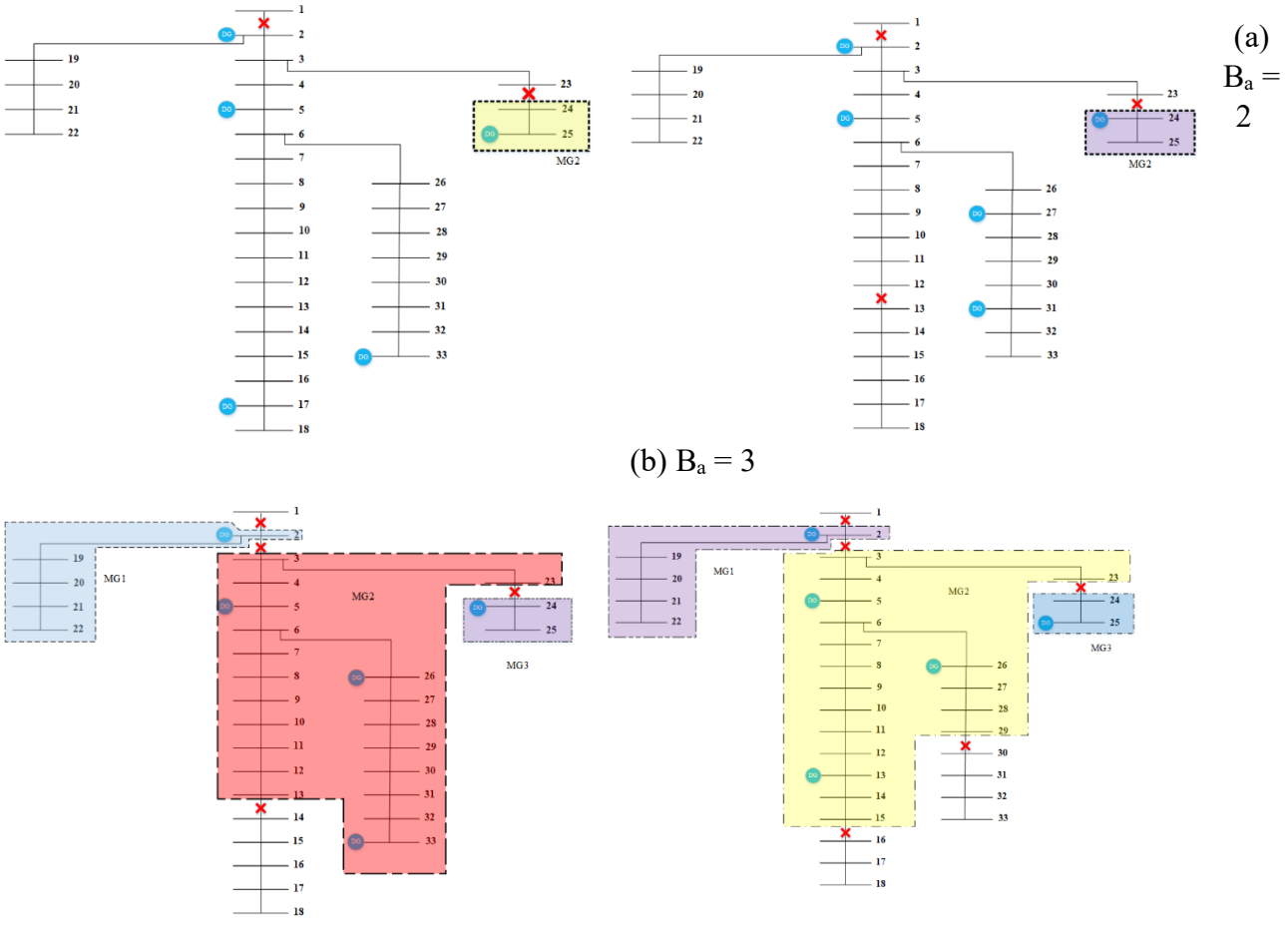

(a) B_a = 2

(b) B_a = 3

(c) B_a = 4

(d) B_a = 5

Fig. 18. Network status after different scenarios by optimal DG placement (B).

General information about the production of distribution resources in different scenarios as well as the amount of power cut in these scenarios is given in Table 8.

Table 8. The amount of load shedding and the active power output of DGs in the corresponding buses in different scenarios

scenario		The amount of active power generated in the corresponding buses [MW]					load shedding [MW}
Ba=1	Bus number	2	4	5	18	31	**0.71**
	PDG [MW]	0.6	0.6	0.6	0.6	0.6	
Ba=2	Bus number	2	5	17	25	33	**0.71**
	PDG [MW]	0.6	0.6	0.6	0.6	0.6	
Ba=3	Bus number	2	5	24	27	31	**0.71**
	PDG [MW]	0.6	0.6	0.6	0.6	0.6	
Ba=4	Bus number	2	5	24	26	33	**0.85**
	PDG [MW]	0.46	0.6	0.6	0.6	0.6	
Ba=5	Bus number	2	5	13	25	26	**1.03**
	PDG [MW]	0.46	0.42	0.6	0.6	0.6	

Fig. 19 shows a comparison between the networks with DGs fixed locations and the network with the optimal placement of DGs.

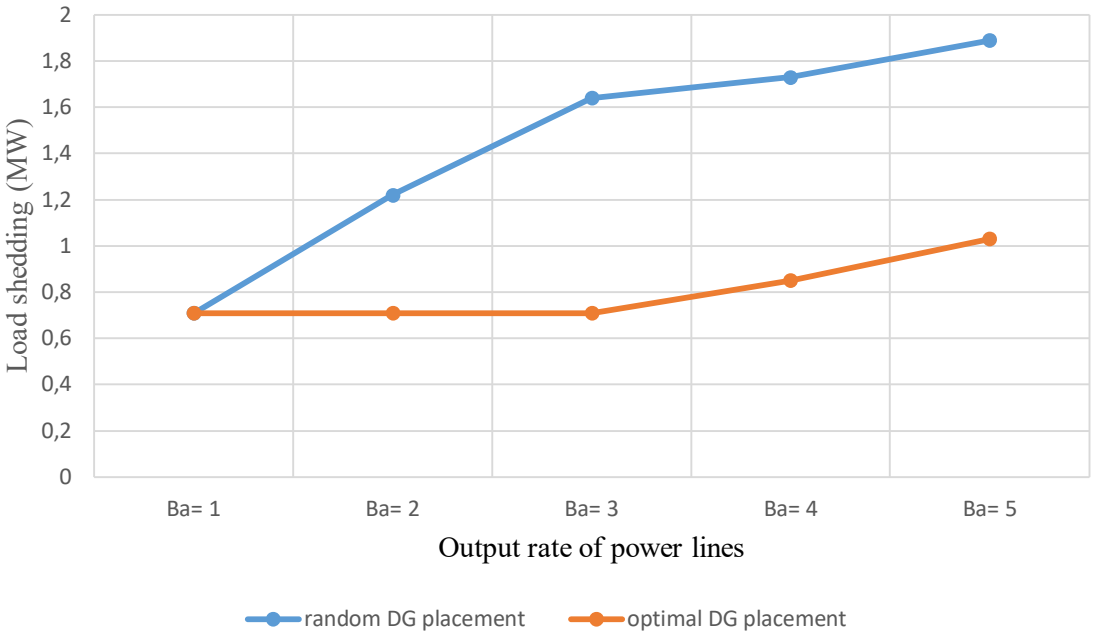

Fig. 19. Comparison of similar scenarios for Model 1 (the mode of without reconfiguration and without hardening) and model 2.

In order to verify the applicability of the proposed approach, we applied it on a larger system namely IEEE 69 bus distribution system [27]. The results obtained for this case study are presented in Table 9. As can be seen, by changing the scenarios, the results are varied because of causing different situations for system operator.

Table 9. The Results obtained for 69-bus system at all scenarios

scenario		Size and Site of DGs [MW]								load shedding [MW]
Ba=1	Bus number	3	5	12	20	33	45	51	58	**1.864**
	PDG [MW]	0.9	1.1	1.1	0.8	0.8	1.5	1.2	1.0	
Ba=2	Bus number	3	6	12	20	30	44	55	65	**1.675**
	PDG [MW]	1.4	1.3	1.2	0.5	0.6	0.9	0.8	1.5	
Ba=3	Bus number	3	5	10	22	35	54	57	68	**1.779**
	PDG [MW]	0.8	0.8	2.1	1.6	1.2	1.2	1.0	1.4	
Ba=4	Bus number	2	7	10	29	38	54	56	63	**2.012**
	PDG [MW]	1.3	1.1	1.1	0.7	0.6	2.1	2.1	1.6	
Ba=5	Bus number	2	5	11	22	30	49	51	66	**2.384**
	PDG [MW]	1.3	1.4	0.8	0.9	0.9	1.2	1.3	1.4	

5. Conclusion

The main goal of electrical energy systems is to provide electricity continuously and with high quality to consumers. Due to climate change caused by greenhouse emissions, the occurrence of destructive accidents is expected to increase in the future, resulting in an increase in the likelihood of damages to the electrical grid and widespread blackouts. Given these conditions, fundamentals beyond the principles of reliability are needed, and as a result, the issue of resilience and its importance is felt more and more. The extension of DGs, MGs forming, and reconfiguration of distribution networks can be used to increase network flexibility to properly cope with severe events. In this paper, we have implemented two models consisting of reinforcement, attack and reconfiguration programs (in the first model) and optimal DG placement (in the second model) to improve the resilience of distribution systems. These models were performed on the 33-bus and 69-bus standard distribution networks under different attack and hardening scenarios. By these models, the following results were obtained:

- By applying reconfiguration in the distribution systems, the amount of load shedding has been significantly reduced compared to non-reconfigurable structure. This comes from network flexibilities that prevent from congestion occurring in the lines.
- The hardening has significantly reduced the amount of load shedding. This is due to the fact that by the reinforcement of the lines, their robustness against events has been increased, therefore, the damages in the network are decreased.
- Simultaneous reconfiguration and hardening will lead to further reduction on the load shedding of the system. Actually, these two schemes complement each other and can make up for each other shortcomings.
- By optimal DG placement, the amount of power cut off is greatly reduced. The DGs act as local backup sources and in island mode provide part of the critical loads of the network. So, they reduce the load shedding of the system when event landfalls.

For the future works, we suggest to consider cutting-edge technologies like mobile energy storages and energy hubs on the proactive management of distribution systems under severe events. Also, the effect of demand response programs and dynamic line rating on the resiliency of the end-user consumers can be considered. Another way to extent the problem is to apply exact uncertainty modelling approaches like IGDT or machine learning to handle the unpredictable nature of severe events.

References

[1] M. Panteli and P. Mancarella, "The Grid: Stronger, Bigger, Smarter? Presenting a Conceptual Framework of Power Systems Resilience," IEEE Power Energy Mag., vol. 13, no. 3, pp. 58–66, 2015.

[2] S. Mousavizadeh, M. R. Haghifam, and M. H. Shariatkhah, "A Linear Two-Stage Method for Resiliency Analysis in Distribution Systems Considering Renewable Energy and Demand Response Resources," Appl. Energy, vol. 211, pp. 443–460, 2018.

[3] Z. Li, M. Shahidehpour, F. Aminifar, A. Alabdulwahab, and Y. Al-Turki, "Networked Microgrids for Enhancing the Power System Resilience," Proc. IEEE, vol. 105, no. 7, pp. 1289–1310, 2017.

[4] J. M. Arroyo, "Bilevel Programming Applied to Power System Vulnerability Analysis under Multiple Contingencies," vol. 4, no. 2, pp. 178–190, 2010.

[5] E. Yamangil, R. Bent, and S. Backhaus, "Designing Resilient Electrical Distribution Grids," 2014.

[6] C. Chen, J. Wang, S. Member, and F. Qiu, "Resilient Distribution System by Microgrids Formation after Natural Disasters," IEEE Transactions on smart grid, vol. 7, no. 2, pp. 958-966, 2015.

[7] W. Yuan et al., "Robust Optimization-Based Resilient Distribution Network Planning Against Natural Disasters," IEEE Transactions on Smart Grid, vol. 7, no. 6, pp. 2817-2826, 2016.

[8] A. Khodaei, "Resiliency-Oriented Microgrid Optimal Scheduling," IEEE Transactions on smart grids, vol. 5, no. 4, pp. 1584–1591, 2014.

[9] H. Gao, S. Member, Y. Chen, and Y. Xu, "Resilience-Oriented Critical Load Restoration Using Microgrids in Distribution Systems," IEEE Transactions on Smart Grid, vol. 7, no. 6, pp. 2837-2848, 2016.

[10] X. Wang, Z. Li, M. Shahidehpour, and C. Jiang, "Robust Line Hardening Strategies for Improving the Resilience of Distribution Systems with Variable Renewable Resources," IEEE Transactions on Sustainable Energy, vol. 10, no. 1, pp. 386-395, 2017.

[11] Y. Lin and Z. Bie, "Tri-level Optimal Hardening Plan for a Resilient Distribution System Considering Reconfiguration and DG Islanding," Appl. Energy, vol. 210, pp. 1266–1279, 2018.

[12] B. Zhang, et al. Robust optimization for energy transactions in multi-microgrids under uncertainty. Applied energy 217: 346-360, 2018.

[13] C. Zhang, Y. Xu, Z. Yang Dong. Probability-Weighted robust optimization for distributed generation planning in microgrids. IEEE Transactions on Power Systems 33(6): 7042-7051, 2018.

[14] Y. Liu, L. Guo, C. Wang. A robust operation-based scheduling optimization for smart distribution networks with multi-microgrids. Applied energy 228: 130-140, 2018.

[15] C. Zhang, et al. Robustly coordinated operation of a multi-energy microgrid with flexible electric and thermal loads. IEEE Transactions on Smart Grid 10(3): 2765-2775, 2018.

[16] H. Qiu, et al. Bi-level two-stage robust optimal scheduling for ac/dc hybrid multi-microgrids. IEEE Transactions on Smart Grid 9(5): 5455-5466, 2018.

[17] B. Zhao, et al. Robust optimal dispatch of ac/dc hybrid microgrids considering generation and load uncertainties and energy storage loss. IEEE Transactions on Power Systems 33(6): 5945-5957, 2018.

[18] H. Qiu, et al. Multi-time-scale rolling optimal dispatch for ac/dc hybrid microgrids with day-ahead distributionally robust scheduling. IEEE Transactions on Sustainable Energy, 2018.

[19] Z. Bie, Y. Lin, G. Li and F.Li, "Battling the Extreme : A Study on the Power System Resilience," Proceedings of the IEEE, vol. 105, no. 7, pp. 1253–1266, 2017.

[20] W. Yuan, L. Zhao, and B. Zeng, "Optimal Power Grid Protection through a Defender – Attacker – Defender model," Reliability. Eng. Syst. Safety, vol. 121, pp. 83–89, 2014.

[21] T. Ding, Y. Lin, S. Member, and G. Li, "A New Model for Resilient Distribution Systems by Microgrids Formation," IEEE Transactions on Power Systems, vol. 32, no. 5, pp. 4145–4147, 2017.

[22] Balakrishnan R, Ranganathan K. A Textbook of Graph Theory. New York, NY: Springer New York; 2012.

[23] T. Ding, H. Sun, K. Sun, F. Li, and X. Zhang, "Graph Theory Based Splitting Strategies for Power System Islanding Operation," IEEE Power Energy Soc. Gen. Meet., pp. 1–5, 2015.

[24] T. Ding, Y. Lin, Z. Bie, and C. Chen, “A Resilient Microgrid Formation Strategy for Load Restoration Considering Master-Slave Distributed Generators and Topology Reconfiguration,” Appl. Energy, vol. 199, pp. 205–216, 2017.
[25] L. Zhao and B. Zeng, “An Exact Algorithm for Two-stage Robust Optimization with Mixed Integer Recourse Problems,” pp. 1–16, 2012.
[26] A. Soroudi and T. Amraee, “Decision Making under Uncertainty in Energy Systems : State of the Art,” Renew. Sustain. Energy Rev., vol. 28, pp. 376–384, 2013.
[27] F. S. Gazijahani and J. Salehi, “Robust Design of Microgrids with Reconfigurable Topology under Severe Uncertainty,” IEEE Transaction on Sustainable Energy, vol. 9, no. 2, pp. 559–569, 2018.
[28] J. Z. Zhu, “Optimal Reconfiguration of Electrical Distribution Network Using the Refined Genetic Algorithm,” Electric Power Systems Research, vol. 62, no. 1, pp. 37–42, 2002.